# Funktionelle und molekulare Charakterisierung von Kaliumkanälen in hippocampalen Astrozyten

Inaugural-Dissertation

zur Erlangung des Doktorgrades

der Hohen Medizinischen Fakultät

der Rheinischen Friedrich-Wilhelms-Universität

Bonn

**Johannes Michael Weller**

aus Tübingen

2017

Angefertigt mit der Genehmigung
der Medizinischen Fakultät der Universität Bonn

1. Gutachter: Prof. Dr. Christian Steinhäuser
2. Gutachter: Prof. Dr. Valentin Stein

Tag der Mündlichen Prüfung: 20.4.2017

Aus dem Institut für Zelluläre Neurowissenschaften
Direktor: Prof. Dr. rer. nat. Christian Steinhäuser

Meinen Eltern

## Inhaltsverzeichnis

# 1. Deutsche Zusammenfassung

## 1.1 Abkürzungsverzeichnis

| | |
|---|---|
| 4-AP | 4-Aminopyridin |
| AA | Arachidonsäure |
| ACSF | artificial cerebrospinal fluid – künstlicher Liquor cerebrospinalis |
| ASIC | acid-sensitive ion channel – Familie säureaktivierter Kationenkanäle |
| ATP | Adenosintriphosphat |
| CA1 | cornu ammonis 1 – eine Hippocampusregion nach Lorente de Nó |
| EGFP | enhanced green fluorescent protein – verbessertes grün fluoreszierendes Protein |
| HEPES | Hydroxyethylpiperazinylethansulfonsäure-Puffer |
| hGFAP | human glial fibrillary acid protein – humanes saures Gliafaserprotein |
| K2P | two-pore domain $K^+$ channel – Kaliumkanalfamilie mit 2 Porendomänen |
| Kir | inwardly rectifying $K^+$ channel – Kaliumkanalfamilie mit einwärts gleichrichtenden Eigenschaften |
| LA | α-Linolensäure |
| NBCe1 | electrogenic sodium bicarbonate cotransporter 1 – elektrogener Kotransporter von Natrium und Bikarbonat |
| NHE1 | sodium hydrogen antiporter 1 – Antiporter von Natrium und Wasserstoff |
| RT-PCR | reverse transcriptase-polymerase chain reaction – Reverse-Transkriptase-Polymerasekettenreaktion |
| slm | Stratum lacunosum-moleculare |
| sr | Stratum radiatum |
| TASK | TWIK-related acid-sensitive potassium channel – ein säureaktivierter K2P-Kanal |
| TEA | Tetraethylammoniumchlorid |
| TNP | Trinitrophenol |
| TREK | TWIK-related potassium channel – ein K2P-Kanal |
| TRPV1 | transient receptor potential vanilloid receptor 1 – TRP-Kationenkanalfamilie |
| TWIK | two-pore domain weak inward rectifier potassium channel – ein einwärts gleichrichtender K2P-Kanal |
| ZNS | zentrales Nervensystem |

## 1.2 Einleitung

Astrozyten sind der numerisch vorherrschende Zelltyp im Gehirn und sie verfügen über eine Vielzahl von Funktionen, die dem Erhalt der Integrität des zentralen Nervensystems (ZNS) dienen. Durch ihre verzweigte Morphologie mit Bildung eines funktionellen Synzytiums über Gap junctions und ihren engen Kontakt zu Synapsen und Kapillaren stellen sie eine Schlüsselstelle sowohl in der Ionen-, Neurotransmitter- und Metabolithomöostase als auch in der Regulation des zerebralen Blutflusses dar und sie beeinflussen die synaptische sowie neurovaskuläre Signalübertragung (Gordon et al., 2007; Henneberger und Rusakov, 2010; Wallraff et al., 2006).

Ihre genannten homöostatischen Aufgaben erfüllen Astrozyten mit einer Vielzahl von spezifischen transmembranalen Proteinen, den Ionenkanälen. Spezialisierte Ionenkanäle dienen dem Transport von Ionen aus dem intrazellulären in den extrazellulären Raum und umgekehrt. Dieser Transport von Ionen verändert die elektrische Membranspannung und die lokale Ionenkonzentration, im Fall von Protonen entsprechend den intra- bzw. extrazellulären pH-Wert. Für das Verständnis der Funktion von Astrozyten ist eine genauere Kenntnis, wie die Aktivität dieser Ionenkanäle gesteuert wird, von großer Wichtigkeit. Insbesondere Kaliumkanäle haben bei der Aufrechterhaltung des negativen Ruhemembranpotentials und der astrozytären Membranleitfähigkeit eine wichtige Rolle, von der astrozytäre Funktionen wie Kaliumpufferung, pH-Regulation und die Aufnahme von Neurotransmittern abhängen (Olsen und Sontheimer, 2008; Pasler et al., 2007). Große Teile der astrozytären Kaliumleitfähigkeit werden den Familien der einwärtsgleichrichtenden Kaliumkanäle (Kir), insbesonder Kir4.1, und der Kaliumkanäle mit 2 Porendomänen (K2P), insbesondere TWIK-1 und TREK-1, zugeschrieben (Seifert et al., 2009; Zhou et al., 2009). Vor allem K2P-Kanäle verleihen durch ihre komplexe Regulation durch Neurotransmitter, pH-Wert, Druck, mehrfach ungesättigte Fettsäuren oder Lipide den Astrozyten spezifische Eigenschaften. Kir4.1-Kanäle werden von intrazellulärer Ansäuerung inhibiert, während TREK-1 durch extrazelluläre Ansäuerung inhibiert wird (Pessia et al., 2001; Sandoz et al., 2009).

Diese beschriebene homöostatische Rolle von Astrozyten ist unter pathophysiologischen Bedingungen gestört (Verkhratsky und Parpura, 2015). Die Funktion von Astrozyten ist somit für das Verständnis vieler Krankheiten des ZNS von besonderem Interesse. Viele pathophysiologische Prozesse im ZNS, wie z.B. Inflammation, Ischämie,

Trauma und epileptische Anfälle, führen zu einer Azidose des Extrazellulärraumes, die astrozytären Eigenschaften unter diesen Bedingungen und ihre Resilienzmechanismen gegen Azidose sind nicht abschließend geklärt.

Der intrazelluläre pH-Wert wird generell über intrazelluläre Puffersysteme und die Aktivität von Ionentransportern gesteuert. In Astrozyten sind dies NHE1, NBCe1 und vermutlich Bikarbonat-Chlorid-Anionenaustauscher (Steinhäuser et al., 2013). Sinkende extrazelluläre Protonen- und Natriumkonzentration unter ischämischen Bedingungen vermindern die treibende Kraft dieser natriumabhängigen Transportmechanismen und führen zu einer intrazellulären Azidose (Chesler, 2005). In Zellkulturexperimenten führte eine anhaltende – nicht aber eine transiente – extrazelluläre Azidose zu intrazellulärer Azidose und zum Tod von Astrozyten (Nedergaard et al., 1991).

Aktuelle Arbeiten vermuten eine funktionelle astrozytäre Expression von Mitgliedern der durch Ansäuerung aktivierten Kanalfamilien der säuresensitiven Kationenkanäle ASIC sowie der Kationenkanäle TRPV, welche nach einem zu ihrer Entdeckung führenden transienten Rezeptorpotential benannt wurden (Huang et al., 2010). Im ventralen Hirnstamm antworten Astrozyten auf eine Ansäuerung mit Kalziumerhöhung und vesikulärer ATP-Ausschüttung (Kasymov et al., 2013). Weiterhin wurde vorgeschlagen, dass die Inhibition der pH-sensitiven Kir-Kanäle Kir4.1/Kir5.1 durch Ansäuerung oder Applikation von $CO_2$ zu zellulärer Depolarisation führt (Wenker et al., 2010).

Ziel dieser Arbeit ist es, mittels funktioneller und molekularer Analyse den Einfluss von Azidose auf die Funktion von Kaliumkanälen in frisch isolierten Astrozyten des murinen Hippocampus zu untersuchen. Dabei soll insbesondere die Frage beantwortet werden, ob Kanäle der ASIC-, TRPV- und K2P-Familien in Astrozyten durch Ansäuerung aktiviert werden.

## 1.3 Material und Methoden

Die elektrophysiologischen Experimente wurden an 8 bis 12 Tage alten Jungtieren einer transgenen Mauslinie durchgeführt, bei der das grün fluoreszierende Protein EGFP unter dem Promotor des humanen sauren Gliafaserproteins hGFAP und somit auch in Astrozyten exprimiert wird. Zur Gewinnung der Gehirnschnitte wurden die Mäuse betäubt, das Gehirn in HEPES-gepufferter Badlösung präpariert, mit einem Vibratom in

200 - 300 µm dicke koronare Gewebeschnitte geteilt und in mit Carbogen (95% $O_2$, 5% $CO_2$) begastem künstlichem Liquor (ACSF) inkubiert.

Für Messungen an isolierten Zellen wurden Gehirnschnitte in oxygeniertem ACSF mit Papain und L-Cystein für 8-12 min inkubiert, die CA1-Region des Hippocampus herauspräpariert und einzelne Zellen durch mechanische Manipulation herausgelöst.

Für Experimente mit Zellen der aus humanen embryonalen Nierenzellen etablierten Zelllinie HEK-293 wurden diese kultiviert und für eine transiente Expression mit der kodierenden Sequenz des Kir4.1-Kanals transfiziert, die freundlicherweise von Dr. Wang-Eckhardt und Prof. Gieselmann vom Institut für Biochemie und Molekularbiologie der Universität Bonn zur Verfügung gestellt wurde.

Elektrophysiologische Experimente wurden an einem Patch-Clamp-Messplatz durchgeführt. Messungen im Gewebeschnitt erfolgten in einer von carbogenbegasten ACSF durchspülten Messkammer unter optischer Kontrolle durch eine Infrarotkamera. Astrozyten wurden durch ihre Morphologie, transgene Fluoreszenz sowie ihre passive elektrophysiologische Charakteristik identifiziert. Mittels Mikromanipulator, Borosilikatglas-Pipetten und einem Patch-Clamp-Verstärker wurden die Zellen mit Patch-Clamp-Technik in der *whole-cell* Konfiguration untersucht und die Messwerte digital aufgezeichnet.

Messungen an isolierten Astrozyten und HEK-Zellen erfolgten in HEPES-gepufferter Badlösung an einem modifizierten Patch-Clamp-Messplatz, welcher das Einführen der während des Experiments an die Patch-Clamp-Pipette adhärenten Zelle in das Innere der rohrförmigen, mit Badlösung gefüllten modifizierten Badelektrode und somit den Transfer in mit unterschiedlichen Modulatoren versetzte Badlösungen erlaubt. Die Untersuchungen erfolgten bei verschiedenen pH-Werten und unterschiedlichen Kaliumkonzentrationen. Als Ionenkanalmodulatoren wurden Amilorid, 4-Aminopyridin (4-AP), Arachidonsäure (AA), Barium, Capsaicin, α-Linolensäure (LA), Prostaglandin $E_2$, Riluzol, Tetraethylammoniumchlorid (TEA) und Trinitrophenol (TNP) verwendet.

Nach elektrophysiologischer Untersuchung von Astrozyten der CA1-Region mittels Patch-Clamp-Technik wurde die untersuchte Zelle unter optischer Kontrolle aus dem Gewebeschnitt gelöst und der Zellinhalt in die Patch-Clamp-Pipette eingesaugt, der Pipetteninhalt mit DNase und RNaseinhibitor behandelt und eine reverse Transkription

durchgeführt. Anschließend erfolgte eine multiplex Einzelzell-PCR in zwei Runden mit spezifischen Primern und die Produkte wurden mittels Gelelektrophorese identifiziert.
Für semiquantitative RT-PCR wurden die Strata radiatum bzw. lacunosum-moleculare der CA1-Region (relativ neuronenarme Zellschichten des Hippocampus, in denen die apikalen Dendriten der Pyramidenzellen liegen und Schaffer'sche Kollateralen verlaufen bzw. Fasern des entorhinalen Kortex enden) aus 200 µm dicken coronaren Hirnschnitten präpariert, die RNA mit Trizol isoliert und nach Behandlung mit DNase und RNaseinhibitor eine reverse Transkription durchgeführt. Mit der mittels Dynabeads isolierten cDNA wurde anschließend eine semiquantitative RT-PCR durchgeführt. Die molekularbiologischen Experimente wurden durch Dr. Seifert durchgeführt.
Die Auswertung der elektrophysiologischen Messwerte erfolgte unter Berechnung elektrophysiologischer Werte wie Eingangswiederstand, Membranleitfähigkeit und Gleichrichtungsindex. Zur statistischen Analyse wurde bei abhängigen Stichproben ein Student's t-Test und bei multiplen Paarvergleichen eine einfache Varianzanalyse (ANOVA) mit anschließendem Post-hoc-Test nach Tukey durchgeführt. Als Signifikanzniveau wurde $p < 0.05$ gewählt.

### 1.4 Ergebnisse

Bei Experimenten mit kultivierten Astrozyten konnten in angesäuerter Badlösung große einwärtsgerichtete Ströme abgeleitet werden, die Kanälen der ASIC-Familie und TRPV1 zugeschrieben wurden (Huang et al., 2010). Um den Einfluss von niedrigem extrazellulärem pH-Wert auf Astrozyten *in situ* zu untersuchen, führten wir Patch Clamp-Experimente an frisch isolierten hippocampalen Astrozyten durch. Durch die Untersuchung an Einzelzellen wird eine bessere Spannungskontrolle sowie eine Vermeidung der Zellkopplung über Gap Junctions erreicht, außerdem werden sekundäre Einflüsse durch Nachbarzellen oder lokale Ionengradienten im Gewebschnitt und eine Verfälschung der Expressionsmuster wie in Zellkultur vermieden. Unter diesen Bedingungen führte eine Ansäuerung von pH 7.4 auf pH 6.0 zu einer signifikanten Reduktion von einwärts- und auswärtsgerichteten Membranströmen um 15.6 ± 8.1 %, bzw. 15.0 ± 9,2 % gemessen bei einem Membranhaltepotential von - 130 mV bzw. + 20 mV ($n=15$, $p<0.001$, Student's t-Test). Das Ruhemembranpotential von - 63.2 ± 7.8 mV wurde nicht beeinflusst und der Eingangswiederstand leicht erhöht. Bereits bei Ansäuerung auf pH

7.0 oder 6.5 ließ sich dabei eine signifikante Reduktion der Leitfähigkeit nachweisen (pH 7.0: n=4, p=0.01 bei negativem und 0.03 bei positivem Membranhaltepotential; pH 6.5: n=3, p=0.01 bei negativem und <0.01 bei positivem Membranhaltepotential). Die pH-sensitive Stromkomponente wies ein Umkehrpotential von - 69 ± 10 mV auf. Da es in der Nähe des mittels Nernst-Gleichung berechneten Gleichgewichtspotentials für Kalium von - 87 mV liegt, wird diese Stromkomponente vermutlich größtenteils durch Kaliumionen vermittelt, möglicherweise durch die in Astrozyten stark exprimierten Kir4.1 und K2P-Kanäle (Seifert et al., 2009).

Um diese Hypothese zu testen, wurde Kir4.1 in HEK-293 Zellen exprimiert und unter denselben Bedingungen elektrophysiologisch charakterisiert. Bei einem Wechsel von pH 7.4 zu pH 6.0 zeigt sich auch hier eine Reduktion der Membranleitfähigkeit um 7.1 ± 5.3 % bzw. 7.5 ± 3.6 % bei - 130 mV bzw. + 20 mV Membranhaltepotential (n=5, p=0.05 bzw. 0.01, Student's t-Test) sowie eine entsprechende Erhöhung des Eingangswiederstands, während das Ruhemembranpotential nicht verändert wurde. Demzufolge könnte die beschriebene Reduktion der astrozytären Membranleitfähigkeit bei extrazellulärer Ansäuerung durch Kir4.1-Kanäle vermittelt sein.

Da extrazelluläre Azidität möglicherweise weitere Ionenkanäle neben Kir4.1 beeinflusst, wurden letztere mit 100 µM Barium blockiert und anschließend der extrazelluläre pH-Wert von 7.4 auf 6.0 reduziert. Die Applikation von Barium führte zu einer Depolarisation des Ruhemembranpotentials mit Anstieg des Eingangswiederstandes und Reduktion der Membranleitfähigkeit. Die anschließende Reduktion des extrazellulären pH-Wertes führte jedoch zu einer reversiblen signifikanten Vergrößerung der Membranleitfähigkeit um 19 ± 19 % und 14 ± 10 % bei - 130 mV bzw. + 20 mV Membranhaltepotential (n=15, p<0.001, Student's t-Test), während das Ruhemembranpotential sich nicht weiter veränderte. Diese pH-sensitive Stromkomponente zeigte eine leichte Auswärtsgleichrichtung und ein Umkehrpotential von - 65 mV und ist somit vermutlich ebenfalls größtenteils durch Kaliumionen vermittelt.

In den folgenden Experimenten wurde die extrazelluläre Kaliumkonzentration isoosmolar auf 20 mM erhöht, um die pH-evozierte Kaliumleitfähigkeit zu verstärken. Um zu testen, ob die beobachtete Stromkomponente sensitiv für Inhibitoren von spannungsaktivierten Kaliumkanälen ist, wurden Messungen nach Applikation von TEA, 4-AP und Barium durchgeführt. Erneut zeigte sich bei Ansäuerung von pH 7.4 auf pH 6.0 eine reversible

Erhöhung der Membranleitfähigkeit um 21 ± 17 % und 32 ± 24 % bei - 130 mV bzw. + 20 mV Membranhaltepotential (n=18, $p<0.001$, Student's t-Test) mit Erniedrigung des Eingangswiederstandes, während das Ruhemembranpotential unverändert blieb. Die pH-induzierten Membranströme sind somit insensitiv gegenüber den applizierten Inhibitoren spannungsaktivierter Kaliumkanäle. Die pH-aktivierte Stromkomponente zeigte eine Auswärtsgleichrichtung und ein Umkehrpotential von - 40 mV, welches in der Nähe des für diese Bedingungen berechneten Gleichgewichtspotential von Kalium (- 47 mV) lag.

Um zu klären, ob Mitglieder der Ionenkanalfamilie ASIC zur pH-abhängigen Leitfähigkeit beitragen, wurde der ASIC-Inhibitor Amilorid in Gegenwart von Barium bei pH 6.0 appliziert. Es zeigte sich jedoch keine Änderung der Membranleitfähigkeit (n=7). Es wurde gezeigt, dass ASIC1a-vermittelte Ströme durch extrazelluläres Kalzium inhibiert werden und nur eine transiente Leitfähigkeit auftritt, sie möglicherweise also daher bei diesem Experiment nicht nachweisbar waren (Waldmann et al., 1997). Deshalb wurden frisch isolierte Astrozyten in normaler und kalziumfreier Badlösung mit einem modifizierten Patch-Clamp-System sehr schnell (<100ms) gegenüber saurem pH exponiert, es konnte jedoch keine transiente Änderung der Membranleitfähigkeit beobachtet werden (n=6).

TRPV1-Kanäle werden von polymodalen nozizeptiven Neuronen exprimiert und sind sensitiv für verschiedene Stimuli wie z.B. Hitze > 43 °C, Capsaicin und saurer pH (4.5 - 5.0) (Julius, 2013). Um TRPV1-vermittelte Ströme in Astrozyten nachzuweisen, wurde Capsaicin in Gegenwart von 4AP, TEA und Barium appliziert. Es zeigte sich keine Änderung der Membranleitfähigkeit (n=7).

Weiterhin wurde die Transkription der Ionenkanäle ASIC1a, ASIC2 und TRPV1 und -2 in Astrozyten mittels Einzelzell-RT-PCR durchgeführt. Es ließ sich keine ASIC1a und ASIC2-kodierende mRNA in Astrozyten nachweisen, während ASIC1a und ASIC2 in Pyramidenneuronen aus CA1 häufig nachgewiesen werden konnte. TRPV1 wurde von hippocampalen Astrozyten ebenfalls nicht exprimiert, TRPV2 selten. Zur Kontrolle des astrozytären Zelltyps diente die Koexpression von S100β.

Die Strom-Spannungskennlinie der pH-aktivierten Membranleitfähigkeit ähnelt den Arachidonsäure (AA)-aktivierten TREK-1-vermittelten Strömen in Astrozyten (Seifert et al., 2009). TREK-1 wird u.a. bei intrazellulärer Ansäuerung und durch mehrfach

ungesättigte Fettsäuren (PUFA) aktiviert (Honore, 2007). Um zu untersuchen, ob extrazelluläre Ansäuerung und PUFA dieselben Kaliumkanäle aktivieren, wurde α-Linolensäure (LA) und AA unter denselben Messbedingungen (20 mM Kalium) in Gegenwart von TEA, 4-AP und Barium, welche TREK-1 nicht inhibieren, appliziert. LA führte zu einer reversiblen Vergrößerung der Membranleitfähigkeit um 31 ± 26 % und 72 ± 50 % bei - 130 mV bzw. + 20 mV Membranhaltepotential (n=8, p=0.01 bzw. <0.01, Student's t-Test) und die evozierten Ströme zeigten ein Umkehrpotential von - 30 mV sowie eine Auswärtsgleichrichtung. Die Applikation von AA ergab ein ähnliches Ergebnis (n=8, p<0.01, Student's t-Test). Prostaglandin E2, ein Stoffwechselprodukt von AA, welches TREK-1 nicht aktiviert, hatte jedoch keinen Einfluss auf die Membranleitfähigkeit (n=10) (Maingret et al., 2000). Trinitrophenol (TNP) wird aufgrund seiner positiven Ladung vor allem in die äußere Schicht der Zellmembran eingelagert und bewirkt durch seine sterische Konformation eine Membrankrümmung und somit eine mechanische Aktivierung von TREK-1-Kanälen (Miller et al., 2003). Applikation von TNP führte ebenfalls zu einer Vergrößerung der astrozytären Membranströme (n=8, p<0.01, Student's t-Test). Riluzol ist ein weiterer Aktivator von TREK-1 und führte ebenfalls zu einer Vergrößerung der astrozytären Membranströme (n=9, p=0.04 bei negativem bzw. <0.01 bei positivem Membranhaltepotential, Student's t-Test). Es wurde gezeigt, dass Chinin (engl.: quinine) K2P-Kanäle wie TREK-1 inhibiert (Lesage und Lazdunski, 2000). Die astrozytären, durch niedrigen extrazellulären pH, LA, TNP und Riluzol evozierten Membranströme waren chininsensitiv (pH: n=7, p=0.02; LA: n=3, p=0.03; TNP: n=3, p=0.01 bei negativem bzw. 0.02 bei positivem Membranhaltepotential; Riluzol: n=4, p<0.01; Student's t-Test). Zusammenfassend legen diese Daten nahe, dass niedriger extrazellulärer pH-Wert TREK-1-Kanäle in hippocampalen Astrozyten aktiviert.

Mittels Einzelzell-RT-PCR erfolgte die Untersuchung der Expression auf Transkriptionsebene von K2P-Kanälen in hippocampalen Astrozyten und Neuronen. TASK1 und TASK3 sind säuresensitive K2P-Kanäle, die durch extrazelluläre Ansäuerung inhibiert werden. Während beide von Pyramidenneuronen der CA1-Region exprimiert werden, ließ sich TASK1 in Astrozyten nicht und TASK3 nur selten nachweisen. Die Bestimmung des Zelltyps erfolgte neben der genannten elektrophysiologischen und morphologischen

Charakterisierung mittels Nachweis der Expression von Kir4.1 bzw. Synaptophysin als Marker für Astrozyten bzw. Neurone.

Weiterhin wurde die Regulation der Expression der in hippocampalen Astrozyten exprimierten K2P-Kanäle TWIK-1, TREK-1 und TREK-2 während der postnatalen Gehirnentwicklung untersucht (Seifert et al., 2009). mRNA wurde aus Gewebsproben der hippocampalen CA1-Region isoliert und semiquantitative real-time RT-PCR mit β-Actin als Referenzgen durchgeführt. Es erfolgten Messungen der Expression im Zeitraum postnataler Tag 3 bis 60, bei denen sich eine Steigerung der Expression von TWIK-1 und TREK-1 während der ersten 3 Wochen mit einem Maximum an Tag 21 nachweisen ließ. TREK-2 zeigte keine Hochregulation und wurde im Vergleich dazu an Tag 21 etwa 10fach geringer exprimiert.

Beim Vergleich zwischen den Subregionen von CA1 Stratum lacunosum-moleculare (slm) und Stratum radiatum (sr) ab Tag 10 zeigte sich eine höhere Expression von TWIK-1 im slm als im sr, ab Tag 21 galt dies auch für TREK-1. Während TWIK-1 ab Tag 10 in beiden Subregionen eine Hochregulation aufwies, galt dies bei TREK-1 nur für das slm. Es konnte also ein Unterschied in der entwicklungsabhängigen Expression gezeigt werden: während TWIK-1 eine Hochregulation in der CA1-Region erfährt, gilt dies für TREK-1 nur im slm, TREK-2 hingegen zeigte keine Hochregulation.

## 1.5 Diskussion

Die pH-Sensitivität von Astrozyten ist ein Resultat vieler beteiligter Mechanismen und großer lokalisationsspezifischer Heterogenität unterworfen. Astrozyten exprimieren eine Vielzahl von Ionentransportern und -austauschern, die den intrazellulären pH-Wert regulieren (Steinhäuser et al., 2013). Sie reagieren dabei auf extrazelluläre Gegebenheiten und tragen damit in verschiedenen Bereichen des ZNS in unterschiedlicher Weise zur Homöostase physiologischer Zustände bei. Im ventralen Hirnstamm beispielsweise antworten Astrozyten auf pH-Senkung und $CO_2$-Steigerung mit einer Erhöhung des intrazellulären Kalzium und der Freisetzung von ATP, wodurch über Aktivierung von Neuronen des retrotrapezoiden Kern (RTN) die Atmung moduliert wird (Gourine et al., 2010). Bei kortikalen Astrozyten konnte dies nicht beobachtet werden (Kasymov et al., 2013). Der Mechanismus, wie es zur geschilderten Erhöhung des intrazellulären Kalziums kommt, ist noch nicht geklärt. Möglicherweise tragen Kir4.1/Kir5.1-

Heteromere dazu bei, indem sie durch pH-abhängige Inhibierung in Astrozyten des RTN eine Depolarisation bewirken (Wenker et al., 2010). In unseren Experimenten mit frisch isolierten hippocampalen Astrozyten hingegen ließ sich keine pH-abhängige Depolarisation nachweisen, was einen weiteren Beleg der lokalisationsspezifischen Heterogenität von astrozytärer pH-Sensitivität darstellt.

Wie bereits geschildert spielt Azidose bei vielen pathophysiologischen Prozessen eine Rolle. Auf zellulärer Ebene führt eine prolongierte Applikation von niedrigem extrazellulärem pH in kultivierten Astrozyten zu einem Abfall des intrazellulären pH-Wertes und bei prolongierter Exposition zeit- und dosisabhängig zum Zelltod (Nedergaard et al., 1991). Ein niedriger intrazellulärer pH-Wert beeinflusst Glykolyse, Kalziumhomöosthase, enzymatische Aktivität und Gap Junctions und kann ebenfalls zum Zelltod führen (Siesjo et al., 1993). Unsere Experimente zeigen eine Reduktion der astrozytären Kaliumleitfähigkeit bei transienter Azidifikation, vermutlich durch Modulation von Kir4.1-Kanälen. Nach Blockade von Kir4.1 verstärkte eine Azidifikation jedoch die verbleibende Kaliumleitfähigkeit. Die hier nachgewiesene Kaliumleitfähigkeit, die insensitiv gegenüber klassischen Blockern spannungsgesteuerter Kaliumkanäle war und im Folgenden thematisiert wird, scheint somit einen Teil der Kir4.1-Modulation auszugleichen. Die Zusammensetzung astrozytärer Kaliumkanäle im Hippocampus erlaubt so die Tolerierung transienter Azidifikation unter Aufrechterhaltung der Kaliumleitfähigkeit und des Ruhemembranpotentials, was für die astrozytäre Homöosthase relevant ist.

K2P-Kanäle stellen eine Familie von derzeit 15 bekannten Isoformen dar, die durch verschiedenste Stimuli reguliert werden und das Ruhemembranpotential entscheidend beeinflussen (Enyedi und Czirjak, 2010). Es wurde vermutet, dass neben Kir4.1 auch die K2P-Kanäle TWIK-1 und TREK-1 zur großen Kaliumleitfähigkeit von Astrozyten beitragen und u.a. TWIK-1 und TREK-1 heteromere Kanäle bilden können (Hwang et al., 2014; Levitz et al., 2016; Seifert et al., 2009; Zhou et al., 2009). Unsere Ergebnisse bestätigen eine funktionelle Expression von TREK-1 und zeigen eine parallele Hochregulation von TREK-1 und TWIK-1-mRNA im Hippocampus. Das maximale Expressionslevel wurde an Tag 21 erreicht, was sich mit den Ergebnissen von Transkriptom- und Proteinanalysen deckt (Cahoy et al., 2008; Wang et al., 2013). Die Expression von Kir4.1 geht etwa eine Woche voraus (Seifert et al., 2009).

Zerebrale Ischämie führt zu einer verstärkten TREK-1-Expression und es wurde vermutet, dass chininsensitive Kaliumkanäle, unter anderem TREK-1, die Proliferation stimulieren (Wang et al., 2011). In Zellkultur führt die Inhibition von TREK-1-Kanälen zu einer reduzierten Glutamatclearance. S100β, auch als damage-associated pattern protein bezeichnet, wird von Astrozyten exprimiert und bei Hypoxie freigesetzt. Zusätzliche Blockade von TREK-1-Kanälen steigerte die Freisetzung von S100β (Wu et al., 2013). Dies weist darauf hin, dass TREK-1 bei Hypoxie aktiv ist, durch Hyperpolarisation möglicherweise zur Homöostase beiträgt und somit die Freisetzung von S100β reduziert. Lu et al. (2013) zeigten, dass TREK-1-vermittelte Ströme in kultivierten Astrozyten sensitiv für AA, niedrigen intrazellulären pH und Unterdruck – vermutlich durch Membrankrümmung – sind. In unseren Experimenten zeigten frisch isolierte Astrozyten ein ähnliches pharmakologisches Profil unter der Annahme, dass die Änderung des extrazellulären pH-Wertes den intrazellulären pH-Wert beeinflusste (Chesler, 2005; Nedergaard et al., 1991). *In vivo* ist die Regulation des intrazellulären pH-Wertes komplexer, denn Hypoxie führt zu massiven Änderungen der transmembranösen Ionengradienten. Demzufolge können Ergebnisse mit isolierten Zellen oder Zellkulturen nur einige Aspekte von systemischer Ischämie wiedergeben und weiterführende Untersuchungen über die Rolle von TREK-1 *in vivo* sind notwendig.

Unsere Studie weist bei transienter Verringerung des extrazellulären pH-Wertes Ströme nach, die aufgrund des pharmakologischen Profils TREK-1 zuzuordnen sind. Chu et al. (2010) wiesen durch niedrigen extrazellulären pH-Wert evozierte, Chinin-insensitive Ströme in Astrozyten nach und vermuteten, dass diese durch einen unbekannten Kaliumkanal vermittelt werden. Möglicherweise ist die Inhibition von K2P-Kanälen bei pH 5 aufgrund der Diprotonierung des tertiären Stickstoffatoms reduziert. Wir beobachteten einen Verlust der Chininsensitivität der Kaliumleitfähigkeit bei einem pH-Wert < 6 und folgern, dass die Ergebnisse von Chu et al. eine funktionelle Expression von TREK-1 in Astrozyten nicht ausschließen.

Zusammenfassend bestätigen und erweitern die vorliegenden Ergebnisse die Daten über funktionelle Expression von TREK-1 in Astrozyten (Hwang et al., 2014; Seifert et al., 2009; Zhou et al., 2009). Wir konnten zeigen, dass diese glialen Ionenkanäle durch AA, Azidifizierung und TNP, welches eine Zellschwellung imitiert, aktiviert werden, also durch Bedingungen, wie sie bei zerebraler Ischämie auftreten. TREK-1 ist möglicher-

weise bei Astrogliose nach zerebraler Ischämie beteiligt und Hypoxie oder akute zerebrale Ischämie führen zu einer Hochregulation von TREK-1 und zu astrozytärer Proliferation (Wang et al., 2011). Die systemische Gabe von Riluzol und α-Linolensäure nach experimentellem Verschluss der Arteria cerebri media konnte Infarktvolumen, DNA-Fragmentierung und Zellschaden reduzieren, wobei die zugrundeliegenden Mechanismen und der primär beteiligte Zelltyp unklar sind (Heurteaux et al., 2006). Ähnlich wie Kir-Kanäle trägt TREK-1 zur passiven astrozytären Membranleitfähigkeit und zum negativen Ruhemembranpotential bei, von dem Funktionen wie Kalium-pufferung, Aufnahme von Neurotransmittern und pH-Regulation abhängen (Olsen und Sontheimer, 2008; Pasler et al., 2007). Eine weitere Aufklärung der TREK-1-vermittelten neuroprotektiven Mechanismen birgt möglicherweise Ansatzpunkte zur Therapie bei zerebraler Ischämie.

ASIC sind eine natrium- und in geringerem Ausmaß auch kalziumpermeable Subfamilie der ENaC/degenerin-Kanalgruppe, die von niedrigem pH geöffnet werden (Kellenberger und Schild, 2015). Im peripheren Nervensystem werden sie vor allem von nozizeptiven Neuronen exprimiert. Die Expression von ASIC im ZNS wurde ebenfalls nachgewiesen (Alvarez de la Rosa et al., 2003). Man vermutet, dass neuronale Aktivität durch ASIC pH-abhängig reguliert wird und eine wichtige Rolle von neuronalen ASIC in azidose-vermittelter Hirnschädigung wie z.B. bei Ischämie konnte nachgewiesen werden (Xiong et al., 2008). Nach der Expression von ASIC in Oligodendrozyten und NG2-Gliazellen wurde nun die Expression von ASIC1 in kultivierten Astrozyten beschrieben (Huang et al., 2010). In unseren Experimenten mit frisch isolierten Astrozyten ließ sich ASIC1 jedoch weder funktionell noch auf Transkriptebene nachweisen, während wir in Kontroll-untersuchungen eine stabile Expression in Pyramidenneuronen der CA1-Region bestätigen konnten. Neben der astrozytären Heterogenität ist eine weitere mögliche Erklärung der widersprüchlichen Ergebnisse zum Nachweis von ASIC in Astrozyten die unterschiedliche Präparationstechnik. Zur Aufrechterhaltung der Hirnparenchymhomöo-stase müssen Astrozyten sensibel auf Milieuänderungen reagieren. Eine profunde Änderung des Transkriptionsmusters durch die Zellkultur scheint plausibel, während die frische Isolation von Einzelzellen Experimente nur im Zeitraum von 1,5 bis maximal 8 Stunden nach Präparation des Tieres erlaubt und dadurch deutlich weniger Änderungen auf Transkriptionsebene zu erwarten sind.

TRPV1 wurde vor allem in primär nozizeptiven Neuronen nachgewiesen. Es bildet einen unspezifischen protonenpermeablen Kationenkanal, der von Stimuli wie Hitze, Säuren, intrazellulärer Alkalose und Substanzen wie Capsaicin aktiviert wird (Dhaka et al., 2009; Hellwig et al., 2004). Im Hippocampus wurde TRPV1 in präsynaptischen Neuronen der CA1-Region nachgewiesen, wo es zur synaptischen Depression beiträgt, und im Gyrus dentatus vermittelt TRPV1 die synaptische Depression durch GABAerge Neurone auf Körnerzellen (Chávez et al., 2014; Gibson et al., 2008). Weiterhin wurde TRPV1 in kultivierten kortikalen Astrozyten und in retinalen Astrozyten nachgewiesen (Ho et al., 2014; Huang et al., 2010). Immunhistochemisch wurde TRPV1 von Toth et al. (2005) in astrozytären Endfüßen und Perizyten im Hippocampus, von Mannari et al. (2013) in astrozytären Endfüßen in den circumventrikulären Organen und von Doly et al. (2004) in Astrozyten des spinalen Hinterhorns nachgewiesen. TRPV1-mRNA konnte auch in kultivierten humanen Astrozten bestätigt werden (Amantini et al., 2007). In unseren Experimenten hingegen waren hippocampale Astrozyten insensitiv gegenüber Capsaicin und TRPV1-mRNA konnte mittels Einzelzell-RT-PCR nicht nachgewiesen werden. Unterschiedliche Präparationstechniken können auch hier möglicherweise die abweichenden elektrophysiologischen Ergebnisse erklären, da ein Verlust eines Teils der astrozytären Endfüße im Präparationsprozess der frisch isolierten Astrozyten nicht auszuschließen ist und möglicherweise nur dort lokalisierte Ionenkanäle so erschwert nachweisbar sind. Alternativ könnte die Divergenz als weiterer Beleg der lokalisationsspezifischen astrozytären Heterogenität interpretiert werden.

## 1.6 Zusammenfassung

Zusammengefasst führte extrazelluläre Azidifizierung zu einer Reduktion der astrozytären Kaliumleitfähigkeit, vermutlich durch Modulation von Kir4.1-Kanälen. Nach Blockade dieser Kanäle vergrößerte ein niedriger pH-Wert die residuelle Kaliumleitfähigkeit wieder, was durch Modulatoren des K2P-Kanals TREK-1 imitiert wurde, wie auf Seite 40 dargestellt wird. Wir fanden keine Belege für ASIC oder TRPV in hippocampalen Astrozyten. Die Zusammensetzung der astrozytären Kaliumkanäle erlaubt somit die Tolerierung transienter Azidifizierung unter Aufrechterhaltung der Kaliumleitfähigkeit und somit des Ruhemembranpotentials.

## 1.7 Literaturverzeichnis der deutschen Zusammenfassung

Alvarez de la Rosa D, Krueger SR, Kolar A, Shao D, Fitzsimonds RM, Canessa CM. Distribution, subcellular localization and ontogeny of ASIC1 in the mammalian central nervous system. J Physiol 2003; 546: 77-87

Amantini C, Mosca M, Nabissi M, Lucciarini R, Caprodossi S, Arcella A, Giangaspero F, Santoni G. Capsaicin-induced apoptosis of glioma cells is mediated by TRPV1 vanilloid receptor and requires p38 MAPK activation. J Neurochem 2007; 102: 977-990

Cahoy JD, Emery B, Kaushal A, Foo LC, Zamanian JL, Christopherson KS, Xing Y, Lubischer JL, Krieg PA, Krupenko SA, Thompson WJ, Barres BA. A transcriptome database for astrocytes, neurons, and oligodendrocytes: a new resource for understanding brain development and function. J Neurosci 2008; 28: 264-278

Chávez AE, Hernández VM, Rodenas-Ruano A, Chan CS, Castillo PE. Compartment-specific modulation of GABAergic synaptic transmission by TRPV1 channels in the dentate gyrus. J Neurosci 2014;34: 16621-16629

Chesler M. Failure and function of intracellular pH regulation in acute hypoxic-ischemic injury of astrocytes. Glia 2005; 50: 398-406

Chu KC, Chiu CD, Hsu TT, Hsieh YM, Huang YY, Lien CC. Functional identification of an outwardly rectifying pH- and anesthetic-sensitive leak K(+) conductance in hippocampal astrocytes. Eur J Neurosci 2010; 32: 725-735

Dhaka A, Uzzell V, Dubin AE, Mathur J, Petrus M, Bandell M, Patapoutian A. TRPV1 is activated by both acidic and basic pH. J Neurosci 2009; 29: 153-158

Doly S, Fischer J, Salio C, Conrath M. The vanilloid receptor-1 is expressed in rat spinal dorsal horn astrocytes. Neurosci Lett 2004; 357: 123-126

Enyedi P, Czirják G. Molecular background of leak K+ currents: two-pore domain potassium channels. Physiol Rev 2010; 90: 559-605

Gibson HE, Edwards JG, Page RS, Van Hook MJ, Kauer JA. TRPV1 channels mediate long-term depression at synapses on hippocampal interneurons. Neuron 2008; 57: 746-759

Gordon GRJ, Mulligan SJ, MacVicar BA. Astrocyte control of the cerebrovasculature. Glia 2007; 55:1214-1221

Gourine AV, Kasymov V, Marina N, Tang F, Figueiredo MF, Lane S, Teschemacher AG, Spyer KM, Deisseroth K, Kasparov S. Astrocytes control breathing through pH-dependent release of ATP. Science 2010; 329: 571-575

Hellwig N, Plant TD, Janson W, Schäfer M, Schultz G, Schaefer M. TRPV1 acts as proton channel to induce acidification in nociceptive neurons. J Biol Chem 2004; 279: 34553-34561

Henneberger C, Rusakov DA. Synaptic plasticity and Ca2+ signalling in astrocytes. Neuron Glia Biol 2010; 3: 141-146

Heurteaux C, Laigle C, Blondeau N, Jarretou G, Lazdunski M. Alpha-linolenic acid and riluzole treatment confer cerebral protection and improve survival after focal brain ischemia. Neuroscience 2006; 137: 241-251

Ho KW, Lambert WS, Calkins DJ. Activation of the TRPV1 cation channel contributes to stress-induced astrocyte migration. Glia 2014; 62: 1435-1451

Huang C, Hu ZL, Wu WN, Yu DF, Xiong QJ, Song JR, Shu Q, Fu H, Wang F, Chen JG. Existence and distinction of acid-evoked currents in rat astrocytes. Glia 2010; 58: 1415-1424

Hwang EM, Kim E, Yarishkin O, Woo DH, Han KS, Park N, Bae Y, Woo J, Kim D, Park M, Lee CJ, Park JY. A disulphide-linked heterodimer of TWIK-1 and TREK-1 mediates passive conductance in astrocytes. Nat Commun 2014; 5: 3227

Julius D. TRP channels and pain. Annu Rev Cell Dev Biol 2013; 29: 355-384

Kasymov V, Larina O, Castaldo C, Marina N, Patrushev M, Kasparov S, Gourine AV. Differential sensitivity of brainstem versus cortical astrocytes to changes in pH reveals functional regional specialization of astroglia. J Neurosci 2013; 33: 435-441

Kellenberger S, Schild L. International Union of Basic and Clinical Pharmacology. XCI. structure, function, and pharmacology of acid-sensing ion channels and the epithelial Na+ channel. Pharmacol Rev 2015; 67: 1-35

Lesage F, Lazdunski M. Molecular and functional properties of two-pore-domain potassium channels. Am J Physiol Renal Physiol 2000; 279: F793-F801

Levitz J, Royal P, Comoglio Y, Wdziekonski B, Schaub S, Clemens DM, Isacoff EY, Sandoz G. Heterodimerization within the TREK channel subfamily produces a diverse family of highly regulated potassium channels. Proc Natl Acad Sci U S A 2016; 113: 4194-4199

Lu L, Wang W, Peng Y, Li J, Wang L, Wang X. Electrophysiology and pharmacology of tandem domain potassium channel TREK-1 related BDNF synthesis in rat astrocytes. Naunyn Schmiedebergs Arch Pharmacol 2014; 387: 303-312

Maingret F, Lauritzen I, Patel AJ, Heurteaux C, Reyes R, Lesage F, Lazdunski M, Honoré E. TREK-1 is a heat-activated background K(+) channel. EMBO J 2000; 19: 2483-2491

Mannari T, Morita S, Furube E, Tominaga M, Miyata S. Astrocytic TRPV1 ion channels detect blood-borne signals in the sensory circumventricular organs of adult mouse brains. Glia 2013; 61: 957-971

Miller P, Kemp PJ, Lewis A, Chapman CG, Meadows HJ, Peers C. Acute hypoxia occludes hTREK-1 modulation: re-evaluation of the potential role of tandem P domain K+ channels in central neuroprotection. J Physiol 2003; 548: 31-37

Nedergaard M, Goldman SA, Desai S, Pulsinelli WA. Acid-induced death in neurons and glia. J Neurosci 1991; 11: 2489-2497

Olsen ML, Sontheimer H. Functional implications for Kir4.1 channels in glial biology: from K+ buffering to cell differentiation. J Neurochem 2008; 107: 589-601

Päsler D, Gabriel S, Heinemann U. Two-pore-domain potassium channels contribute to neuronal potassium release and glial potassium buffering in the rat hippocampus. Brain Res 2007; 1173: 14-26

Pessia M, Imbrici P, D'Adamo MC, Salvatore L, Tucker SJ. Differential pH sensitivity of Kir4.1 and Kir4.2 potassium channels and their modulation by heteropolymerisation with Kir5.1. J Physiol 2001; 532: 359-367

Sandoz G, Douguet D, Chatelain F, Lazdunski M, Lesage F. Extracellular acidification exerts opposite actions on TREK1 and TREK2 potassium channels via a single conserved histidine residue. Proc Natl Acad Sci U S A 2009; 106: 14628-14633

Seifert G, Hüttmann K, Binder DK, Hartmann C, Wyczynski A, Neusch C, Steinhäuser C. Analysis of astroglial K+ channel expression in the developing hippocampus reveals a predominant role of the Kir4.1 subunit. J Neurosci 2009; 29: 7474-7488

Steinhäuser C, Seifert G, Deitmer JW. Physiology of astrocytes: Ion channels and transporters. In: Kettenmann H, Ransom B, eds. Neuroglia. (3rd ed.). New York: Oxford University Press, 2013

Siesjö BK, Katsura K, Mellergård P, Ekholm A, Lundgren J, Smith ML. Acidosis-related brain damage. Prog Brain Res. 1993; 96: 23-48

Tóth A, Boczán J, Kedei N, Lizanecz E, Bagi Z, Papp Z, Edes I, Csiba L, Blumberg PM. Expression and distribution of vanilloid receptor 1 (TRPV1) in the adult rat brain. Brain Res Mol Brain Res 2005; 135: 162-168

Verkhratsky A, Parpura V. Astrogliopathology in neurological, neurodevelopmental and psychiatric disorders. Neurobiol Dis 2016; 85: 254-261

Waldmann R, Champigny G, Bassilana F, Heurteaux C, Lazdunski M. A proton-gated cation channel involved in acid-sensing. Nature 1997; 386: 173-177

Wallraff A, Köhling R, Heinemann U, Theis M, Willecke K, Steinhäuser C. The impact of astrocytic gap junctional coupling on potassium buffering in the hippocampus. J Neurosci 2006; 26: 5438-5447

Wang M, Song J, Xiao W, Yang L, Yuan J, Wang W, Yu Z, Xie M. Changes in lipid-sensitive two-pore domain potassium channel TREK-1 expression and its involvement in astrogliosis following cerebral ischemia in rats. J Mol Neurosci 2012; 46: 384-392

Wang W, Putra A, Schools GP, Ma B, Chen H, Kaczmarek LK, Barhanin J, Lesage F, Zhou M. The contribution of TWIK-1 channels to astrocyte K(+) current is limited by retention in intracellular compartments. Front Cell Neurosci 2013; 7: 246

Wenker IC, Kréneisz O, Nishiyama A, Mulkey DK. Astrocytes in the retrotrapezoid nucleus sense H+ by inhibition of a Kir4.1-Kir5.1-like current and may contribute to chemoreception by a purinergic mechanism. J Neurophysiol 2010; 104: 3042-3052

Wu X, Liu Y, Chen X, Sun Q, Tang R, Wang W, Yu Z, Xie M. Involvement of TREK-1 activity in astrocyte function and neuroprotection under simulated ischemia conditions. J Mol Neurosci 2013; 49: 499-506

Xiong ZG, Pignataro G, Li M, Chang SY, Simon RP. Acid-sensing ion channels (ASICs) as pharmacological targets for neurodegenerative diseases. Curr Opin Pharmacol 2008; 8: 25-32

Zhou M, Xu G, Xie M, Zhang X, Schools GP, Ma L, Kimelberg HK, Chen H. TWIK-1 and TREK-1 are potassium channels contributing significantly to astrocyte passive conductance in rat hippocampal slices. J Neurosci 2009; 29: 8551-8564

## 2. Publikation

# pH-Sensitive $K^+$ Currents and Properties of $K_2P$ Channels in Murine Hippocampal Astrocytes

**Johannes Weller, Christian Steinhäuser[1], Gerald Seifert**
Institute of Cellular Neurosciences, Medical Faculty, University of Bonn, Bonn, Germany
[1]Corresponding author: e-mail address: christian.steinhaeuser@ukb.uni-bonn.de

## Contents



*Advances in Protein Chemistry and Structural Biology*, Volume 103
ISSN 1876-1623
http://dx.doi.org/10.1016/bs.apcsb.2015.10.005

## Abstract

Based on their intimate spatial association with synapses and the capillary, astrocytes are critically involved in the control of ion, transmitter, and energy homeostasis as well as regulation of the cerebral blood flow. Under pathophysiological conditions, dysfunctional astrocytes can no longer assure homeostatic control although the underlying mechanisms are poorly understood. Specifically, neurological diseases are often accompanied by acidification of the extracellular space, but the properties of astrocytes in such an acidic environment are still a matter of debate. To meet the homeostatic requirements, astrocytes are equipped with intercellular gap junctions, inwardly rectifying $K^+$ (Kir) channels, and two-pore domain $K^+$ ($K_2P$) channels. One goal of the present study was to overview current knowledge about astrocyte $K^+$ channel function during acidosis. In addition, we combined functional and molecular analyses to clarify how low pH affects $K^+$ channel function in astrocytes freshly isolated from the developing mouse hippocampus. Extracellular acidification led to a decrease of $K^+$ currents in astrocytes, probably due to modulation of Kir4.1 channels. After blocking Kir4.1 channels, low pH enhanced $K^+$ current amplitudes. This current activation was mimicked by modulators of TREK-1 channels, which belong to the $K_2P$ channels family. We found no evidence for the presence of acid-sensitive ion channels and transient receptor potential vanilloid receptors in hippocampal astrocytes. In conclusion, the assembly of astrocytic $K^+$ channels allows tolerating short, transient acidification, and glial Kir4.1 and $K_2P$ channels can be considered promising new targets in brain diseases accompanied by pH shifts.

## 1. INTRODUCTION

Astrocytes play a key role in brain ion homeostasis and neurotransmitter uptake, thereby modulating synaptic and neurovascular signaling. Of particular interest is the alteration of astrocyte function under pathophysiological conditions. Pathological conditions such as tissue inflammation, cerebral ischemia, trauma, and epileptic seizures lead to acidification of the extracellular space via accumulation of lactic acid and $H^+$, which might render pH regulation of neurons and glial cells difficult (Nedergaard, Goldman, Desai, & Pulsinelli, 1991; reviewed by Siesjo et al., 1993). For example, severe ischemia can reduce the pH of brain parenchyma to 6.0 (Rehncrona, 1985) and under hyperglycemic conditions astrocytic acidosis may reach 1–2 orders of magnitude more acidic values (Kraig & Chesler, 1990). However, astrocytic pathophysiology under acidic conditions remains elusive.

Regulation of intracellular pH is mediated by intracellular pH buffers and the activity of ion transporters and exchangers that may extrude protons. Major pH regulating transport systems expressed in astrocytes are the

$Na^+/H^+$ exchanger NHE1, the electrogenic $Na^+/HCO_3^-$ cotransporter NBCe1, and probably the $HCO_3^-/Cl^-$ anion exchangers (Chesler, 2005; Steinhäuser, Seifert, & Deitmer, 2013). Under ischemic conditions, the fall of extracellular pH and $Na^+$ diminish the driving force for $Na^+$-coupled transporters and exchangers leading to profound intracellular acidification (Chesler, 2005; Rose, Waxman, & Ransom, 1998). In cultured astrocytes, long-lasting exposure to low pH entails irreversible decrease of intracellular pH and cell death (Nedergaard et al., 1991). Extracellular acidification is also accompanied by an almost complete block of gap junctional coupling of astrocytes (Wallraff et al., 2006), rendering $K^+$ buffering insufficient. Recent cell culture work claimed that astrocytes express proton-activated acid-sensitive ion channels (ASICa) and transient receptor potential vanilloid receptors (TRPV1) (Huang et al., 2010). Astrocytes located in the ventral part of the brainstem respond to a decrease of extracellular pH with $Ca^{2+}$ elevation and vesicular ATP release (Kasymov et al., 2013). It was suggested that the inhibition of pH-sensitive inwardly rectifying $K^+$ (Kir) channels Kir4.1/Kir5.1 by acidification or $CO_2$ administration leads to depolarization (Wenker, Kreneisz, Nishiyama, & Mulkey, 2010).

Among the $K^+$ channels identified in the plasma membrane of astrocytes *in situ* after fresh isolation are Kir4.1 channels and the two-pore domain $K^+$ ($K_2P$) channels, Tandem of P-domains in a weakly inward rectifying $K^+$ channel 1 (TWIK-1), and TWIK-related $K^+$ channel 1 (TREK-1) (Seifert et al., 2009; Zhou et al., 2009). Notably, $K_2P$ channels confer new properties to astrocytes as they are regulated by neurotransmitters, pH changes, pressure, polyunsaturated fatty acids (PUFAs), or lipids. Recently, $K_2P$ channels were identified as a release pore for glutamate in astrocytes, and they were shown to form heteromeric channels within the $K_2P$ channel family (Hwang et al., 2014; Woo et al., 2012). Kir4.1 $K^+$ channels are potentially inhibited by acidic intracellular pH (Pessia, Imbrici, D'Adamo, Salvatore, & Tucker, 2001), while TREK-1 channels are inhibited by decrease of extracellular pH (Sandoz, Douguet, Chatelain, Lazdunski, & Lesage, 2009).

In the present work, we wanted to clarify how pH affects ion channel function in the membrane of astrocytes freshly isolated from the hippocampus. Specifically, we asked whether members of the ASIC family, TRPV receptors and $K_2P$ channels are activated through decreasing pH. Freshly isolated astrocytes were employed to improve clamp control, avoid potential culture artifacts, and avoid indirect effects through neighboring cells as inevitable in the slice preparation. Our pharmacological and single-cell transcript

analyses hinted at a prominent expression of TREK-1 while we found no evidence for the presence of acid-sensitive ASICs and TRPV channels. We conclude that the composition of $K^+$ channels in the astrocytic plasma membrane is assembled to tolerate short-time acidification and maintain $K^+$ membrane currents, keeping the negative resting membrane potential relatively unchanged.

## 2. MATERIALS AND METHODS

Mice were kept under standard housing conditions and all experiments were carried out in accordance with local, state, and European regulations.

### 2.1 Acute Slice Preparation of Murine Hippocampi

Transgenic human glial fibrillary acidic protein/enhanced green fluorescent protein (Tg(hGFAP/EGFP)) mice (Nolte et al., 2001) of postnatal day (P) 8 to P12 were anesthetized, sacrificed by decapitation and their brains were dissected, washed, and cut into 300 μm thick coronal slices using a vibratome (VT 1000S; Leica Microsystems). Slice preparation was performed at 6 °C in $Ca^{2+}$-free HEPES-buffered external solution containing (in mM) 150 NaCl, 5 KCl, 2 $MgSO_4$, 10 HEPES, 10 glucose, 1 sodium pyruvate, pH adjusted to 7.38, bubbled with oxygen. Subsequently, slices were stored for at least 30 min in artificial cerebrospinal fluid (ACSF) at 4 °C, containing (in mM) 126 NaCl, 3 KCl, 2 $CaCl_2$, 2 $MgSO_4$, 1.25 $NaH_2PO_4$, 37 $NaHCO_3$, 10 glucose, and 40 sucrose. The solution was gassed with carbogen (95% $O_2$, 5% $CO_2$, pH 7.4).

### 2.2 Preparation of Freshly Isolated Cells

Freshly isolated cells were obtained as described previously (Matthias et al., 2003). Briefly, slices obtained as above were incubated in oxygenated ACSF containing papain (24 U/ml) and L-cysteine (0.24 mg/ml) (8–12 min, room temperature, bubbled with carbogen). After washing, the CA1 region of the hippocampus (strata radiatum and lacunosum-moleculare) was dissected under a stereomicroscope (STEMI 2000; Zeiss), and cells were isolated using tungsten needles and Pasteur pipettes.

## 2.3 HEK-293 Cell Culture and Transfection

HEK-293 cells were maintained in plastic dishes in DMEM with Glutamax and 25 mM glucose (Life Technologies) supplemented with 10% fetal calf serum (PAA Laboratories) and penicillin/streptomycin (PAA Laboratories). For transfection, we incubated 0.4 μg DNA with 2 μl transfection medium (TurboFect; Fermentas) in 100 μl DMEM without supplements in well plates for 20 min, and then HEK cells were transferred on top of the transfection reagent/DNA mixture. Cells were held for 2 days at 37 °C in an incubator (5% $CO_2$). For transient expression, we used the whole coding sequence of the Kir4.1 channel (kindly provided by L. Wang-Eckardt and V. Gieselmann).

## 2.4 Electrophysiological Recordings

For recordings *in situ*, slices were transferred to a recording chamber and continuously perfused with carbogenated standard ACSF containing (in mM): 126 NaCl, 3 KCl, 2 $CaCl_2$, 2 $MgSO_4$, 1.25 $NaH_2PO_4$, 26 $NaHCO_3$, and 10 glucose. Cells were visualized using an upright microscope equipped with an infrared DIC system (Eclipse E600FN, Nikon, Germany) at 60-fold magnification. The infrared image was captured with a CCD camera (COHU; model 4912-5100M; Poway; USA). Whole-cell voltage-clamp experiments were performed on cells identified by endogenous fluorescence. Pipettes fabricated from borosilicate capillaries (Science Products, Germany) had a resistance of 3–6 MΩ when filled with internal solution containing (in mM) 130 KCl, 0.5 $CaCl_2$, 2 $MgCl_2$, 5 BAPTA, 10 HEPES, and 3 $Na_2$-ATP, pH 7.25. Pipette capacitance was compensated for. Currents were recorded using the patch-clamp technique in the whole-cell configuration with an EPC-7 patch-clamp amplifier (HEKA Elektronik, Lambrecht, Germany), filtered at 3 and 10 kHz, digitized with an ITC 16 (NPI electronic), and sampled at 6 and 30 kHz by an interface connected to a computer system, which also served as a stimulus generator. Recordings were monitored with TIDA software (HEKA). Holding potential for experiments in slices was −70 mV.

Experiments on isolated astrocytes and HEK-293 cells employed a customized concentration clamp device connected to an EPC-7 amplifier and TIDA software (Seifert & Steinhäuser, 1995). Cells were recorded in HEPES-buffered external solution containing (in mM) 150 NaCl, 5 KCl, 2 $CaCl_2$, 2 $MgCl_2$, 10 glucose, 10 HEPES, pH adjusted to 7.38. Visual

control was achieved with an inverted microscope (Zeiss Axiovert 135) equipped with conventional bright-field DIC. Holding potential for experiments with isolated cells was −60 mV. All recordings were performed at 23–25 °C. Ion channel modulators and blockers were applied by transferring the isolated cell with a tube electrode to the different solutions. Concentrations of ion channel modulators and blockers were as follows: 100 μM amiloride (AMI), 4 mM 4-aminopyridine (4-AP), 10 μM arachidonic acid (AA), 100 μM $BaCl_2$, 100 μM capsaicin (CAP), 10 μM α-linolenic acid (LA), 10 μM prostaglandin $E_2$ ($PGE_2$), 100 μM riluzole (RIL), 10 mM tetraethylammonium chloride (TEA), 0.4 mM trinitrophenol (TNP). All reagents were purchased form Sigma unless stated otherwise. AMI, AA, CAP, LA, $PGE_2$, RIL, and TNP were suspended in DMSO (final concentration 0.05–0.2%), aliquoted, and added to bath solution immediately before use. For experiments in elevated $K^+$ (20 mM), HEPES-buffered external solution consisted of (in mM) 121 NaCl, 20 KCl, 2 $CaCl_2$, 2 $MgCl_2$, 10 Glucose, 10 HEPES, 10 TEA, 4 4-AP, 0.1 $Ba^{2+}$.

## 2.5 Cell Harvesting and Single-Cell RT-PCR

After recording of astrocytes in the stratum radiatum (sr) of the hippocampal CA1 region *in situ*, the cell content was carefully sucked into the recording pipette under optical control with a CCD camera (COHU) using IR-DIC optics. The pipette content was transferred to a tube filled with 3 μl of DEPC-treated water, frozen in liquid nitrogen, and stored at −20 °C. Single-cell transcript analysis was performed as reported (Matthias et al., 2003; Seifert, Rehn, Weber, & Steinhäuser, 1997). Briefly, reverse transcription (RT, 37 °C, 1 h) was performed by adding first-strand buffer (Life Technologies), dithiothreitol (DTT; 10 mM), dNTPs (4 × 250 μM; Life Technologies), RNasin (20 U; Promega), random hexamer primers (50 μM; Roche), and reverse transcriptase (SuperscriptIII; 100 U; Life Technologies). For detection of TASK1 and TASK3 mRNA, DNaseI digestion was performed prior to the RT reaction (Seifert et al., 2009).

A multiplex two-round single-cell PCR was performed with primers for ASICs, TRPVs, Kir4.1, and subunits of the $K_2P$ channel family (see Table 1). The first PCR was performed after adding PCR buffer, $MgCl_2$ (2.5 mM), primers (200 nM each), and 5 U of Taq polymerase (Life Technologies) to the RT product (final volume, 50 μl). Forty-five cycles were performed (denaturation at 94 °C, 25 s; annealing at 49 °C, 2 min for the first five cycles, and 45 s for the remaining cycles; extension at 72 °C,

**Table 1** Primers for Single-Cell RT-PCR

| Gene | Sequence | Position | Product Length (bp) | GeneBank Accession No. |
|---|---|---|---|---|
| ASIC1a/2 | se 5′-AACGGGCTGGAGATCATGCTGGAC<br>as 5′-AGGGCTGGGTCTGCACACTCCTT | 796, 646<br>1171, 1021 | 389 | NM_007384, NM_009597 |
| ASIC1a/2 (nested) | se 5′-GTGGCTCCAGGSTTCCAGACSTT<br>as 5′-CCATGCGGCAGTTGCAGTTYTCCA | 943, 793<br>1103, 953 | 184 | |
| TRPV1 | se 5′-TGCCCTATCATCACCGTCAGC<br>as 5′-AGTGCCATGTTCCGCCTTTCAAT | 217<br>628 | 434 | NM_001001445 |
| TRPV1 (nested) | se 5′-CGCCCCCAAGGCTCTATGAT<br>as 5′-GCCTTTCAATGGCAATGTGTA | 323<br>617 | 316 | |
| TRPV2 | se 5′-TTTCCCGAAAGTTCACCGAGTGGT<br>as 5′-ACCCCCAAGCAGGATCAGAATGTG | 962<br>1297 | 359 | NM_011706 |
| TRPV2 (nested) | se 5′-ACCGCATGGTGGTTTTAGAGC<br>as 5′-AAGTCGCTTTTGATGAGGGAATGG | 1094<br>1247 | 177 | |
| TASK1 | se 5′-TTCTACTTCGCCATCACCGTCATC<br>as 5′-AGAAAGTCCAGCGCTCGTAGTAGG | 250<br>536 | 310 | NM_010608 |

*Continued*

**Table 1** Primers for Single-Cell RT-PCR—cont'd

| Gene | Sequence | Position | Product Length (bp) | GeneBank Accession No. |
|---|---|---|---|---|
| TASK1 (nested) | se 5′-CTTCGCCATCACCGTCATCACCAC<br>as 5′-CGCATGCCCAGCCCCCTCTT | 255<br>449 | 195 | |
| TASK3 | se 5′-AGCCGAAGAAGTCCGTCTCAGAGG<br>as 5′-CAGCCGCCCCAAGGCACAGG | 126<br>510 | 404 | NM_001033876 |
| TASK3 (nested) | se 5′-AAATTCGCCGGTTCCTTCTAC<br>as 5′-GCCACAGCACTTCTTGATACG | 235<br>424 | 210 | |
| Synaptophysin | se 5′-AGGTGCTGCAGTGGGTCTTT<br>as 5′-TCTGGCGGCACATAGGCATCT | 89<br>539 | 471 | NM_009305 |
| Synaptophysin (nested) | se 5′-CGGCTGAGCGTGGAGTGTGC<br>as 5′-AGGGCCCCCATGGAGTAGAGGAA | 154<br>346 | 215 | |
| S100 β | se 5′-AGGCCATGGTTGCCCTCATTGAT<br>as 5′-ACTCATGGCAGGCCGTGGTCA | 17<br>242 | 246 | NM_009115 |
| S100β (nested) | se 5′-TACTCCGGGCGAGAGGGTGACAA<br>as 5′-GGCGACGAAGGCCATGAACTCC | 52<br>216 | 186 | |

"Se" and "as" mark sense and antisense primers. Position 1 is the first nucleotide of the initiation codon. All sense and antisense primers except those for TASK1 and TASK3 are located on different exons, respectively.

25 s; final elongation at 72 °C, 7 min). An aliquot (2 μl) of the PCR product was used as a template for the second PCR (35 cycles; annealing at 54 °C, 2 min for the first five cycles, and 45 s for the remaining cycles) using nested primers (Table 1). The conditions were the same as described for the first round, but dNTPs (4 × 50 μM) and Platinum Taq polymerase (2.5 U; Invitrogen) were added. Products were identified with gel electrophoresis using a molecular weight marker (low-molecular-weight marker; New England Biolabs). As a positive control, RT-PCR for single cells and for total RNA from mouse brain were run in parallel. Negative controls were performed using distilled water or bath solution for RT-PCR.

## 2.6 Preparation of Brain Tissue for Semiquantitative RT-PCR

Tissue samples were isolated from 200 μm thick coronal brain slices. By using a stereo microscope, the strata radiatum and lacunosum-moleculare of the CA1 region were isolated with a small scalpel by removing strata pyramidale and oriens. For regional comparison, in some cases, the radiatum of the CA1 region was further separated from the lacunosum-moleculare and underwent sqRT-PCR analysis. At each developmental stage, at least three mice from different litters were used. Total RNA was isolated from tissue samples with Trizol (Invitrogen) and dissolved in 10 μl DEPC-treated water. Genomic DNA was removed with DNase treatment in a mixture containing PCR buffer, 2.5 mM $MgCl_2$, 10 mM DTT (all Life Technologies), 20 U DNaseI (Roche), and 40 U RNase inhibitor (Promega; final volume 20 μl; incubation at 37 °C for 30 min). Subsequently, mRNA was isolated using oligo$(dT)_{25}$-linked Dynabeads (Life Technologies) and the adherent mRNA was suspended in DEPC-treated water (20 μl). RT (37 °C, 1 h) was performed by adding a mastermix containing first-strand buffer (Life Technologies), dithiothreitol (DTT; 10 mM), dNTPs (4 × 250 μM; Life Technologies), RNasin (40 U; Promega), random hexamer primers (50 μM; Roche), and reverse transcriptase (SuperscriptIII; 200 U; Invitrogen, final volume 40 μl). Semiquantitative PCR was performed in a reaction volume of 12.5 μl. The reaction mixture contained TaqMan™ mastermix and the primers/probe mix (Life Technologies). One-microliter cDNA from the RT product was added to each well. PCRs for $K_2P$ channel subunits and β-actin were run in separate wells. Negative controls (water) were also performed in each run. Samples were incubated at 50 °C (2 min), and after denaturation (95 °C, 10 min), 50 cycles were performed (denaturation at 94 °C, 15 s; primer annealing and extension at 60 °C, 60 s). Fluorescence intensity was readout during each annealing/extension step.

## 2.7 Data Analysis

Membrane capacitance and series resistance were determined offline using IGOR software. Membrane conductance was calculated by dividing membrane current through the corresponding driving force at −130 and +20 mV. The rectification index (RI) was determined by comparing the chord conductances of blocker-sensitive and modulator-evoked currents at −40 and −130 mV (in standard solution):

$$\mathrm{RI} = \frac{I_{(-40\ \mathrm{mV})}}{(-40\ \mathrm{mV} - E_{\mathrm{rev}})} \Big/ \frac{I_{(-130\ \mathrm{mV})}}{(-130\ \mathrm{mV} - E_{\mathrm{rev}})} \tag{1}$$

or at 0 and −90 mV (20 mM $K^+$ solution):

$$\mathrm{RI} = \frac{I_{(0\ \mathrm{mV})}}{-E_{\mathrm{rev}}} \Big/ \frac{I_{(-90\ \mathrm{mV})}}{(-90\ \mathrm{mV} - E_{\mathrm{rev}})} \tag{2}$$

where $I$ is the amplitude of the respective currents, and $E_{\mathrm{rev}}$ its extrapolated reversal potential.

The KCNK/β-actin gene expression ratio was determined by comparing $C_{\mathrm{T}}$ values of the target gene with those of the reference gene, β-actin. The relative quantification of different genes was determined according to the following equation:

$$\begin{aligned} &R_n = X \times E^{\mathrm{CT}} \text{ or, in the logarithmic form,} \\ &\log Y = \log X + C_{\mathrm{T}} \times \log E \end{aligned} \tag{3}$$

with $R_n$ being the fluorescence intensity, $X$ the input copy number, $E$ the efficiency of amplification, and $C_{\mathrm{T}}$ the cycle number at threshold. By quantification of KCNK gene expression against that of β-actin, $C_{\mathrm{T}}$ was determined for each gene at the same $R_n$ and the difference in input copy number was estimated according to Eq. (4):

$$\frac{X_{\mathrm{KCNK}}}{X_{\beta-\mathrm{actin}}} = \frac{E_{\beta-\mathrm{actin}}{}^{\mathrm{CT}_{\beta-\mathrm{actin}}}}{E_{\mathrm{KCNK}}{}^{\mathrm{CT}_{\mathrm{KCNK}}}} \tag{4}$$

The amplification efficiency was 1.73, 1.70, 1.74, and 1.76 for KCNK1, KCNK2, KCNK10, and β-actin, respectively.

Statistical significance ($p < 0.05$) was calculated using Student's $t$-test for paired data or ANOVA followed by TUKEY's post-hoc test.

# 3. RESULTS

## 3.1 Effect of Acidic Extracellular pH on Astrocytic Membrane Currents

Recent work on cultured astrocytes demonstrated large inward currents upon application of bath solution with a pH of 6.0. These currents were thought to be mediated by acid-sensitive channels of the ASIC family and transient receptor potential channel vanilloid type I (TRPV1) (Huang et al., 2010). To test whether low pH inhibits $K^+$ channels and elicits channel/receptor-mediated inward currents *in situ*, we performed patch-clamp experiments on astrocytes isolated from the hippocampus of Tg(hGFAP/EGFP) mice. Astrocytes were identified through their EGFP fluorescence, morphology, and passive current pattern (Matthias et al., 2003). Upon acidification of bath solution to pH 6.0, we observed a significant reduction of outward (to 85.0 ± 9.2%, $V = +20$ mV) and inward currents (to 84.4 ± 8.1%, $V = -130$ mV) compared to the control obtained at pH 7.4 ($n = 15$). Notably, we did not observe an increase in membrane conductance, which would have indicated expression of acid-sensitive channels or receptors (Fig. 1A). The resting potential (−63.2 ± 7.8 mV; $n = 10$) remained unchanged at pH 6.0 (–62.5 ± 9.3 mV), but the input resistance (46 ± 19 MΩ; pH 7.4) increased (57 ± 26 MΩ; pH 6.0). In the majority of cells, the pH-sensitive currents reversed close to the $K^+$ equilibrium potential (−69 ± 10 mV, $n = 10$; Fig. 1B) indicating that they were mainly carried by $K^+$, possibly through Kir4.1 or $K_2P$ channels, which are strongly expressed by astrocytes in the hippocampus (Seifert et al., 2009). A significant reduction of in- and outward conductance was already obvious at pH 7.0 ($n = 4$) and at pH 6.5 ($n = 3$; not shown).

The pH sensitivity of Kir4.1 channels was tested after stable expression in HEK-293 cells. Similar to astrocytes, switching to bath solution with pH 6.0 did not affect the resting potential of Kir4.1-expressing HEK-293 cells (−68.1 ± 5.7 mV, pH 7.4; −69.5 ± 4.4 mV, pH 6.0) but led to an increase in input resistance (by 8.7 ± 5.2%, $n = 5$) due to a reduction of the membrane conductance at low pH (to 92.9 ± 5.3%, $V = -130$ mV and to 92.5 ± 3.6%, $V = +20$ mV; $n = 5$; not shown). Accordingly, the acidification-induced reduction of astrocytic membrane conductance might have been due to modulation of Kir4.1 channels.

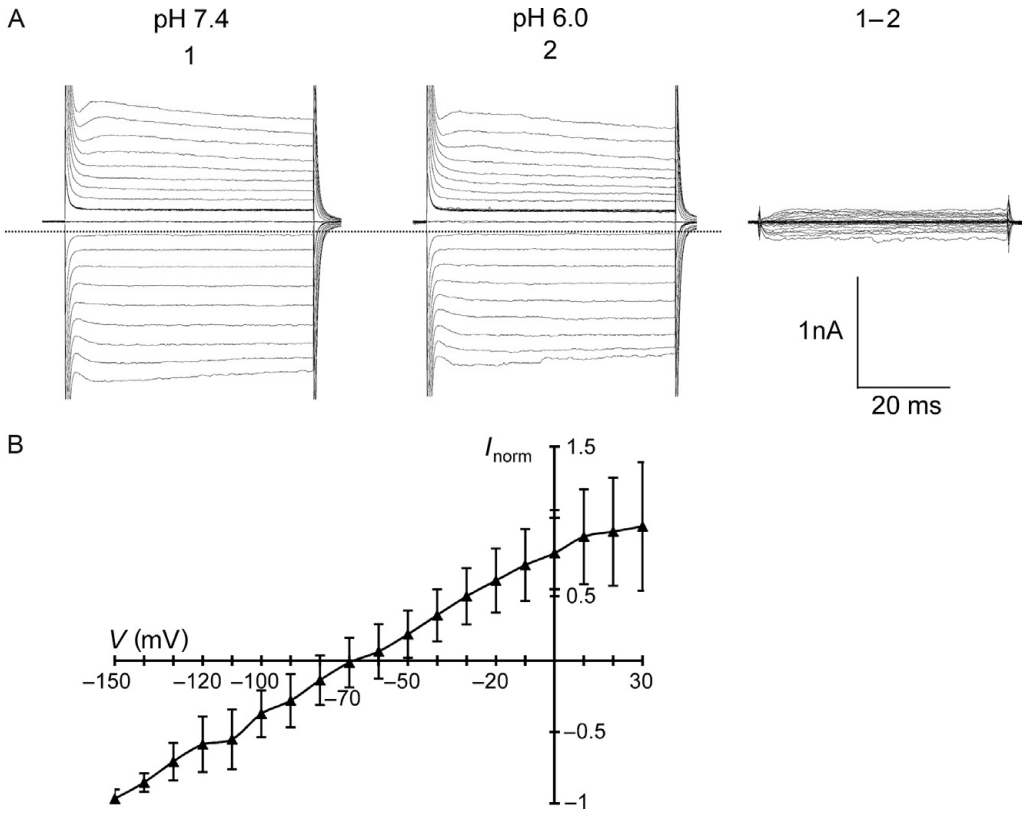


**Figure 1** pH sensitivity of freshly isolated astrocytes. (A) Whole-cell membrane currents were activated in HEPES-buffered solution at pH 7.4 (left panel) and pH 6.0 (middle) by de- and hyperpolarization between −150 and +30 mV (10 mV increment, holding potential –60 mV). Dotted lines indicate zero current. pH-sensitive currents were determined by subtraction of currents at pH 6.0 from those at pH 7.4 (right). (B) *I*/*V*-relation of the pH-sensitive currents as indicated in (A, right panel) ($n = 10$, normalized to maximum inward current in each cell).

## 3.2 Low pH Increases Membrane Currents When Kir4.1 Channels Were Blocked

To test whether acidic pH selectively inhibits Kir4.1 channel-mediated currents in astrocytes, they were blocked with 100 μM $Ba^{2+}$ prior to exposing the cells to bath solution with pH 6.0 and $Ba^{2+}$. After $Ba^{2+}$ application (pH 7.4), the cells' resting potential depolarized (from $-64 \pm 9$ to $-47 \pm 10$ mV, $n = 23$), which was accompanied by an increase in input resistance (from $63 \pm 38$ to $220 \pm 144$ MΩ) and a reduction of membrane conductance (to $63 \pm 26\%$ and $25 \pm 13\%$ at +20 and −130 mV, respectively; Fig. 2A). In the presence of $Ba^{2+}$, acidification (from pH 7.4 to 6.0) did not change resting potential. However, in most cells the membrane conductance significantly increased under these conditions (to $119 \pm 19\%$ and $114 \pm 10\%$ at −130 and +20 mV, respectively; $n = 15/23$). The pH-induced conductance

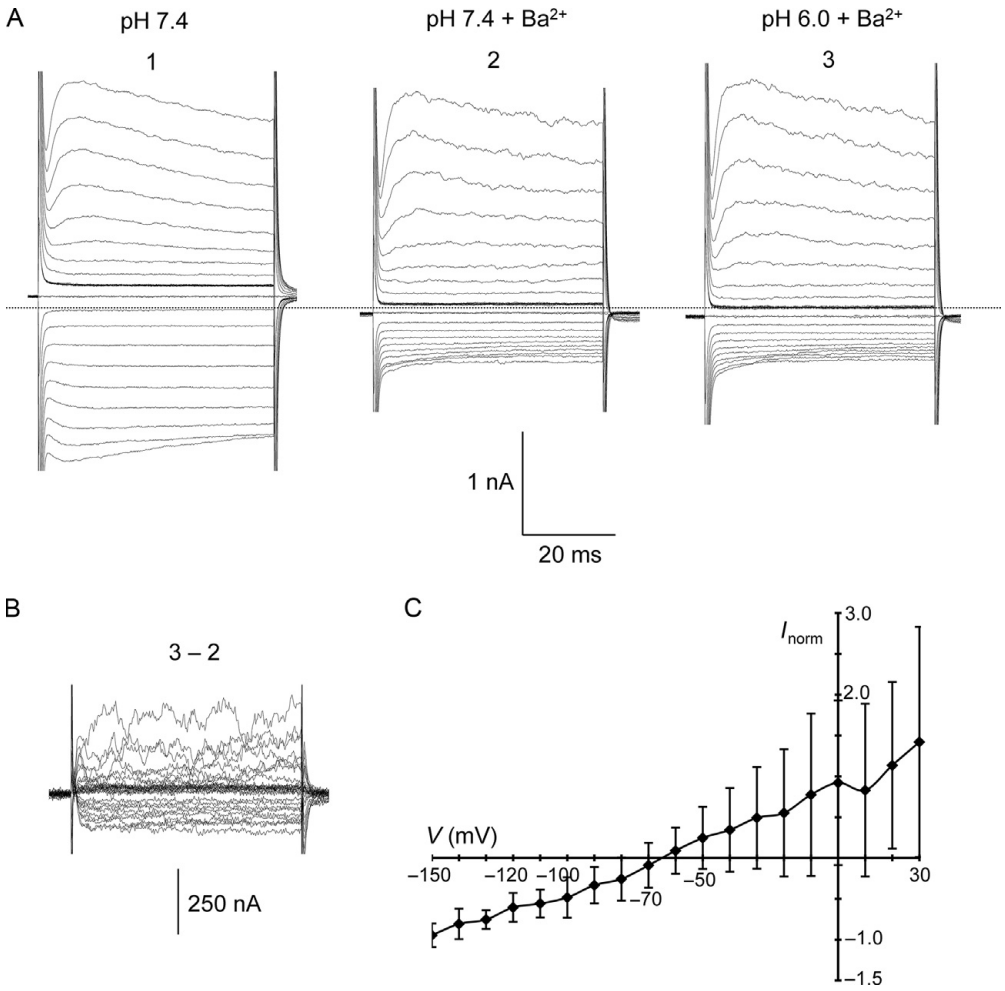


**Figure 2** Low pH elicited membrane currents in the presence of $Ba^{2+}$. (A) Membrane currents were activated as described in Fig. 1A. After evoking control currents (left), HEPES-buffered bath solution supplemented with $Ba^{2+}$ (100 μM) was applied at pH 7.4 (middle) and pH 6.0 (right). (B) The low pH-induced currents were obtained by subtraction of the respective current families. (C) *I*/*V*-relation of the pH 6.0-induced currents as it indicated in (B) ($n = 11$, normalized to maximum inward current in each cell).

increase was reversible when switching back to pH 7.4. This pH-dependent current recorded in the absence of Kir channels reversed at −65 mV and showed weak outward rectification (Fig. 2C).

## 3.3 pH-Induced Membrane Currents Are Insensitive to Blockers of Voltage-Activated $K^+$ Channels

To increase pH-evoked currents, the extracellular $K^+$ concentration was iso-osmolarily raised to 20 mM, which shifted the $K^+$ equilibrium potential to −47 mV. We examined if the low pH-induced conductance is sensitive

to blockers of voltage-activated $K^+$ currents. In presence of tetraethylammonium chloride (TEA, 10 mM), 4-aminopyridine (4-AP, 4 mM), and $Ba^{2+}$ (100 μM) in 20 mM $[K^+]_o$, acidification to pH 6.0 lead to a reversible conductance increase (at +20 mV: 132 ± 24%; at −130 mV: 121 ± 17%; $n = 18$) compared to the control at pH 7.4 (Fig. 3A). Low pH did not affect the resting potential ($V = -34.0 \pm 5.6$ mV and −33.9 ± 6.5 mV at pH 7.4 and 6.0, respectively; $n = 18$) but led to a decrease in input resistance (from 154 ± 108 to 119 ± 75 MΩ). The *I/V* curve of low pH-activated currents in high $K^+$ solution showed outward rectification (RI: 1.43) and reversed direction at −40 mV ($n = 13$), close to the $K^+$ equilibrium potential (Fig. 3B).

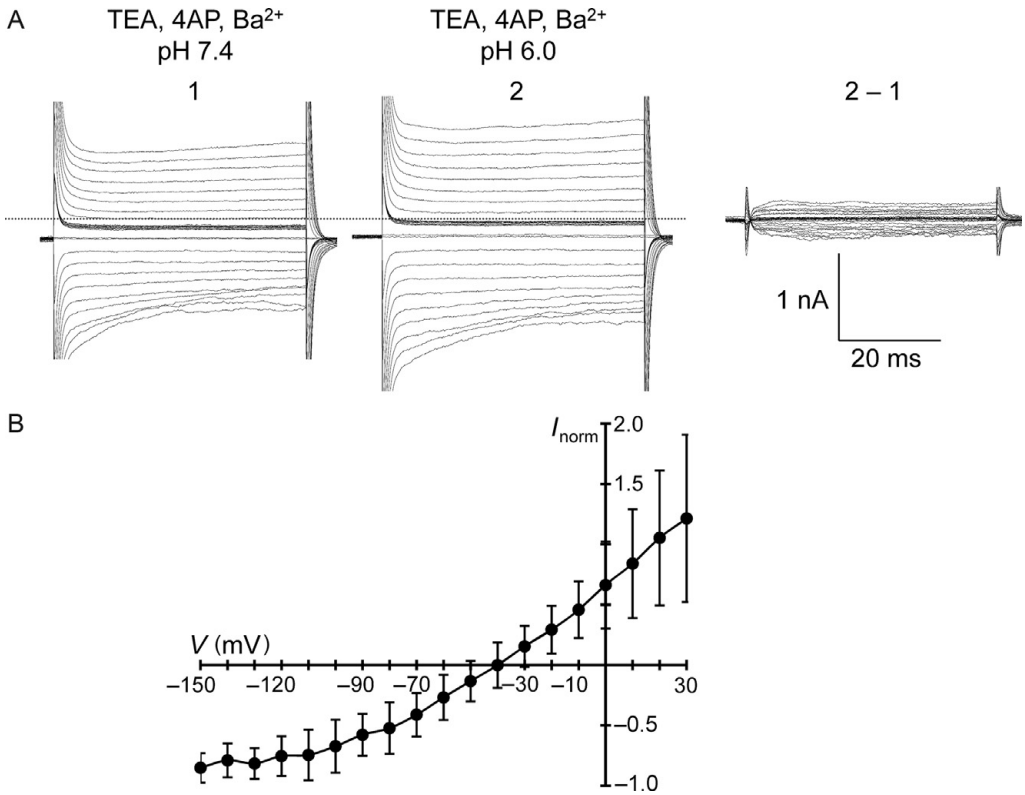


**Figure 3** Low pH extracellular solution evoked outward rectifying membrane currents in the presence of $K^+$ channel blockers. (A) Freshly isolated astrocytes were incubated in bath solution with 20 mM $[K^+]_o$ supplemented with TEA (10 mM), 4-AP (4 mM), and $Ba^{2+}$ (100 μM) and currents were evoked as described in Fig. 1A. After obtaining control currents (left), the pH was switched to pH 6.0 (middle) and low pH-evoked currents were isolated (right). (B) *I/V*-relation of low pH-induced currents ($n = 13$, normalized to the maximum inward current in each cell).

### 3.4 Does Acidic Bath Solution Activate ASIC- or TRPV1-Mediated Currents?

To further evaluate whether ASIC contributed to the conductance activated at acid pH in the presence of $Ba^{2+}$, the ASIC blocker amiloride was added. Amiloride (100 μM) did not affect astrocytic membrane currents (+20 mV: 105 ± 9%; −130 mV: 102 ± 6%; $n = 7$; Fig. 4A). Because ASIC1a-mediated currents have been reported to be transient and inhibited by extracellular $Ca^{2+}$ (Waldmann, Champigny, Bassilana, Heurteaux, & Lazdunski, 1997), astrocytes were rapidly (<100 ms) exposed to pH 6.0 in normal ($n = 4$) and nominally $Ca^{2+}$-free extracellular solution ($n = 6$). No responses were observed under either condition (Fig. 4B).

Acid-sensitive TRPV1 channels are sensitive to various stimuli, expressed by polymodal nociceptive neurons and activated by noxious heat (>43 °C), the pungent vanilloid capsaicin, and acidic pH (4.5–5.0) (Julius, 2013). To test for activation of TRPV1-mediated currents in astrocytes, voltage-activated and Kir currents were blocked as before and the cells were exposed to capsaicin (100 μM; pH 7.4). Capsaicin did not affect the membrane conductance (+20 mV: 92 ± 9%; −130 mV: 100 ± 6%; $n = 7$; Fig. 4C).

To examine expression of ASIC and TRPV1 on the transcript level, we performed single-cell RT-PCR by harvesting the cytoplasm from individual astrocytes and subsequent functional analysis. A two-round PCR was performed, with primers common to ASIC1a and ASIC2 transcripts in the first PCR and gene-specific primers in the second round. None of the astrocytes tested contained mRNAs encoding ASICs ($n = 6$; Fig. 4D). In contrast, ASIC1a and ASIC2 were frequently found in CA1 pyramidal neurons (in 60% and 33% of cells analyzed, $n = 15$; Fig. 4D and E). Similarly, TRPV channels were not or only very rarely expressed by hippocampal astrocytes (TRPV1: $n = 0/7$; TRPV2: $n = 1/7$; Fig. 4D and E). Astrocytes were identified through coexpression of S100β ($n = 13$).

### 3.5 Does Low Extracellular pH Activate $K_2P$ Channels in Astrocytes?

The *I/V* relation of the low pH-activated responses in the presence of TEA, 4-AP, and $Ba^{2+}$ resembled arachidonic acid-induced currents through TREK-1 channels in astrocytes (Seifert et al., 2009). The latter may open upon acidification of the cytoplasm (Honore, 2007). To test whether low pH and PUFAs activate the same $K^+$ channel subunits, we applied linolenic

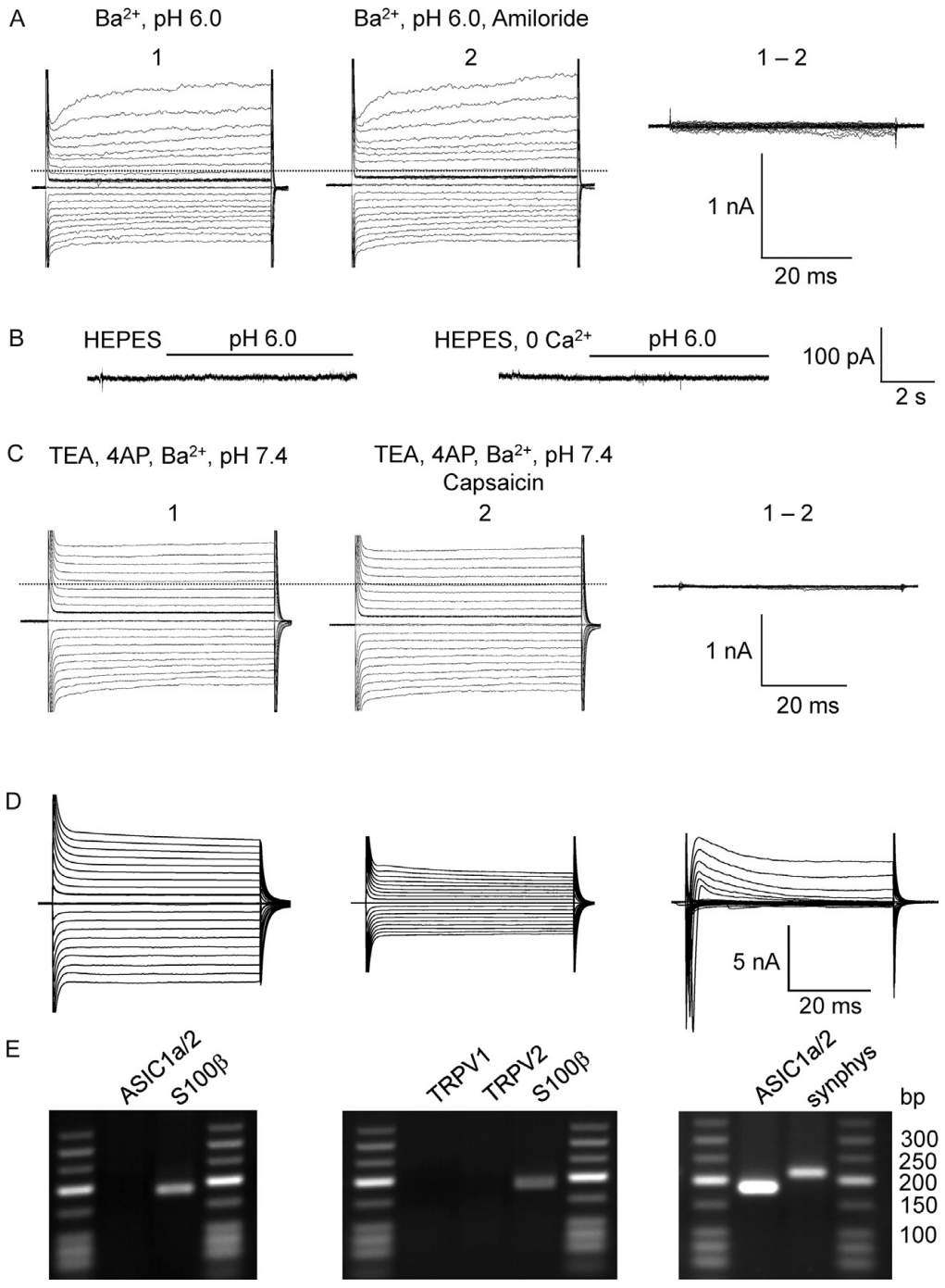


**Figure 4** Freshly isolated astrocytes lack ASICs and TRPV1. (A) Membrane currents were evoked as described in Fig. 1A at pH 6.0 in the presence of $Ba^{2+}$ (100 μM, left) and $Ba^{2+}$ plus amiloride (100 μM each, middle). The responses were insensitive to the ASIC blocker amiloride (right). (B) At a holding potential of −60 mV, bath solution with 2 mM $Ca^{2+}$ (left) and without $Ca^{2+}$ (middle) was fast switched from pH 7.4 to 6.0. (C) Currents were recorded in the presence of $Ba^{2+}$ (100 μM), 4-AP (4 mM), and TEA (10 mM) at pH 7.4, before (left) and after incubation with the TRPV1 agonist capsaicin (100 μM, middle). Subtracting both current families revealed lack of TRPV1.

and arachidonic acid in high extracellular $K^+$ solution (20 mM) in presence of the above $K^+$ channel blockers, which do not inhibit TREK-1 channels. α-Linolenic acid (10 μM) increased the membrane conductance (+20 mV: 172 ± 50%; −130 mV: 131 ± 26%; $n = 8$). The corresponding *I/V* relation reversed at −30 mV and showed outward rectification (RI: 1.7; $n = 7$; Fig. 5A and D). A similar conductance increase was observed after application of arachidonic acid (10 μM; +20 mV: 158 ± 44%; −130 mV: 149 ± 41%; $n = 10$). The *I/V* relation reversed at −35 mV and showed outward rectification (RI: 1.7, $n = 10$; Fig. 5B and D). In contrast, prostaglandin E2 ($PGE_2$, 10 μM), a product of cyclooxygenase-mediated conversion of arachidonic acid that rather inactivates TREK-1 currents (Maingret et al., 2000), left the membrane currents unaffected ($n = 7$; not shown). The membrane crenator trinitrophenol (TNP), another TREK-1-opener (Miller et al., 2003), also activated a conductance (400 μM; +20 mV: 130 ± 17%; −130 mV: 118 ± 8%; $n = 8$). These currents reversed at −26 mV and showed outward rectification (RI: 2.4; $n = 8$; Fig. 5C and D). Eventually, the TREK-1-activator riluzole (100 μM) also enhanced astrocytic membrane currents (+20 mV: 133 ± 22%; −130 mV: 114 ± 20%; $n = 9$; Fig. 5D). The activation of putative $K_2P$ channel-mediated currents was always reversible. The currents evoked by low extracellular pH, PUFAs, TNP, and riluzole were all sensitive to quinine (200 μM), a $K_2P$ channel blocker (Lesage & Lazdunski, 2000) (at +20 mV: pH 6.0 to 71 ± 24%, $n = 7$; α-linolenic acid to 59 ± 15%, $n = 3$; TNP to 30 ± 14%, $n = 3$; riluzole to 43 ± 1%, $n = 4$). A similar decrease of membrane conductance was observed at −130 mV. Together, these data strongly suggest that low pH activates TREK channels in hippocampal astrocytes.

## 3.6 Developmental Upregulation of $K_2P$ Channel mRNA in the Hippocampus

To assess the expression of the acid-sensitive $K_2P$ subunits TASK1 and TASK3, we performed single-cell RT-PCR subsequent to functional

(D) Representative current patterns of astrocytes (left, middle) and a CA1 pyramidal neuron (right). Cells were de- and hyperpolarized *in situ* between −160 and +20 mV (10 mV increment, holding potential −70 mV). (E) After recording, the cytoplasm was harvested and single-cell RT-PCR performed. Astrocytes expressed transcripts for the marker S100β (186 bp) but lacked ASICs and TRPVs (left, middle). In contrast, mRNA-encoding ASIC1/2 (184 bp) was found in synaptophysin-expressing CA1 pyramidal neurons (right).

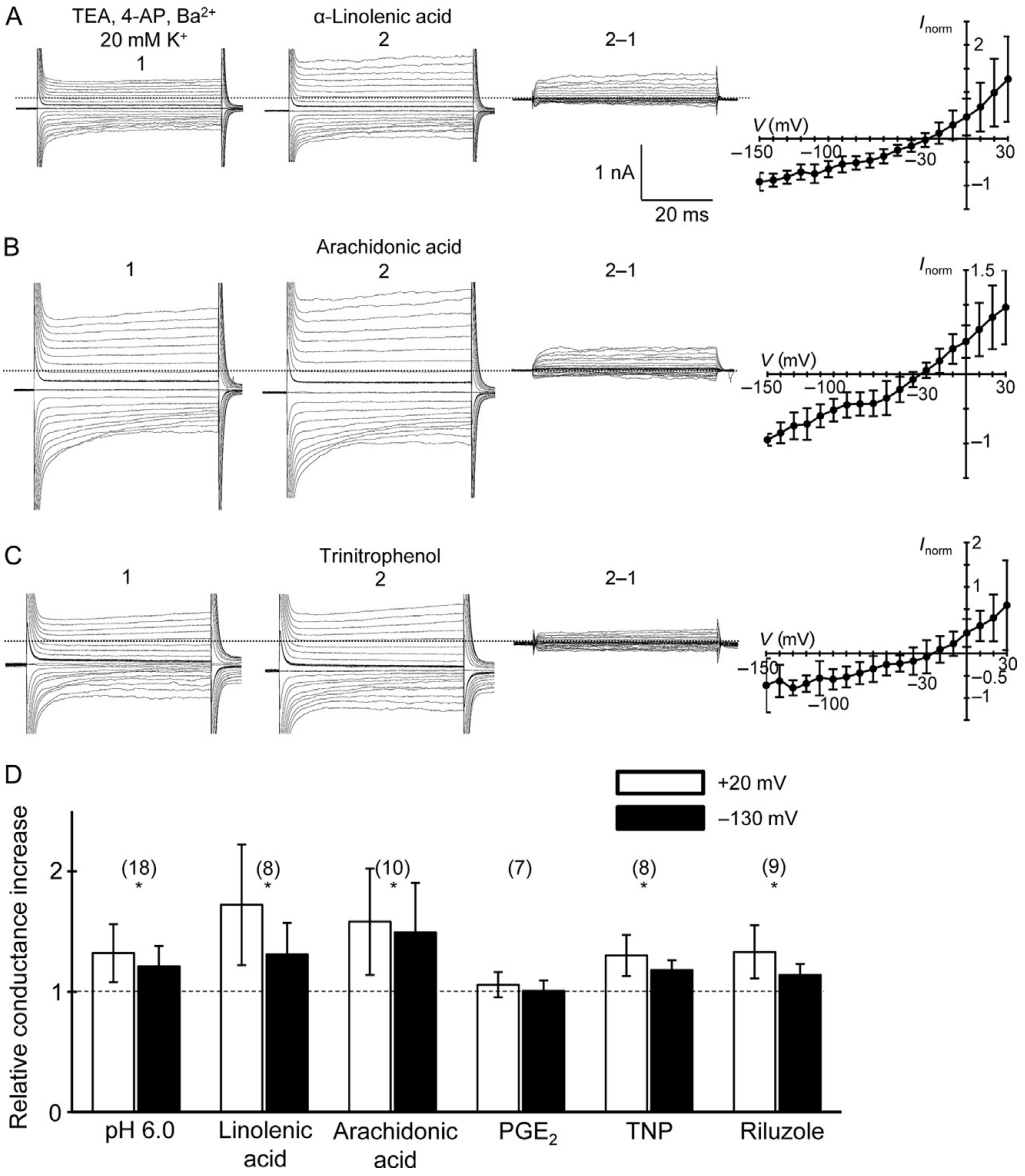


**Figure 5** TREK-1 channel agonists mimic the effect of low pH. (A–C) Currents were activated as described in Fig. 1A in a solution containing 20 mM $K^+$ and the $K^+$ channel blocker TEA (10 mM), 4 AP (4 mM), and $Ba^{2+}$ (100 μM) (left panels). α-Linolenic acid (10 μM), arachidonic acid (10 μM), and trinitrophenol (400 μM) enhanced the responses (second row), which were isolated by subtracting currents at respective voltages (third row). The right panel shows the corresponding *I*/*V*-relations, normalized to maximum inward currents. (D) summarizes the effect of TREK-1 channel modulators at +20 mV (open bars) and −130 mV (filled). The concentrations of $PGE_2$ and riluzole were 10 and 100 μM, respectively. Asterisks indicate significant changes through modulator application at pH 7.4, or after switching the bath solution to pH 6.0. Cell numbers are given in parentheses.

analysis. Both subunits were coexpressed by CA1 pyramidal neurons ($n = 5$). In contrast, astrocytes consistently lacked TASK1 ($n = 12$) and only rarely expressed TASK3 ($n = 1/7$; not shown). For cell type identification, primers for Kir4.1 (astrocytes) and synaptophysin (neurons) were used.

Next, we investigated the developmental regulation of the K2P subunits TWIK-1 (KCNK1), TREK-1 (KCNK2), and TREK2 (KCNK10), which are expressed by hippocampal astrocytes (Seifert et al., 2009). mRNA was isolated from small tissue samples of the hippocampal CA1 region and semi-quantitative real-time RT-PCR was performed. β-actin served as a reference gene. An increase of KCNK1 and KCNK2 expression was observed during the first three postnatal weeks, reaching a maximum at p21 (Fig. 6A left and middle panel, 6B). In contrast, the abundance of KCNK10 was lower by a factor of 10 at p21 and remained constant by p60 (Fig. 6A right panel and 6B).

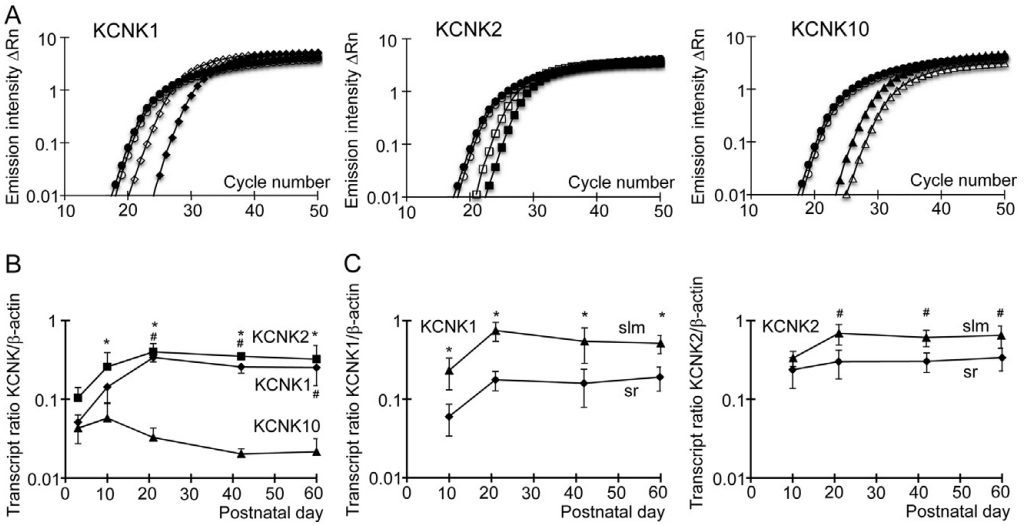


**Figure 6** Developmental regulation of KCNK1, KCNK2, KCNK10 mRNA expression in the CA1 region of hippocampus. (A) Amplification plots for the respective KCNK subunits (diamonds, squares, triangles) and β-actin (circles) from mice at p3 (filled symbols) and p21 (open) using real-time sqRT-PCR. Note that for KNCK1 and KCNK2, the difference in threshold cycles (taken at $\Delta Rn = 0.1$) at p3 exceeded the p21 value. (B) The gene ratios, KCNK/β-actin, were determined according to Eq. (4) and plotted against age. Mean and SD were obtained at p3 to p60 (eight samples each). Differences between p3 and later ages (*) and p10 and later ages (#) were statistically significant. KCNK10 mRNA expression showed no developmental regulation. (C) The ratios KCNK1/β-actin and KCNK2/β-actin were determined and plotted against postnatal age. Higher ratios were observed for stratum lacunosum-moleculare (triangles) versus stratum radiatum (diamonds). Data were obtained from six samples each.

By comparing mRNA expression in CA1 subregions, higher KCNK1 expression was found in the stratum lacunosum-moleculare (slm) versus sr (Fig. 6C left). Similarly, between p21 and p60 KCNK2 mRNA was more abundant in the slm (Fig. 6C right). KCNK1 was upregulated in both subregions between p10 and p20, while KCNK2 expression in the sr remained unchanged (Fig. 6C right).

## 4. DISCUSSION

### 4.1 ASICs and TRPVs in Astrocytes

ASICs comprise a subfamily of the ENaC/degenerin channel family, which are gated by low pH and permeable to $Na^+$ and to a lower extent also to $Ca^{2+}$ (Kellenberger & Schild, 2015). Their expression in the peripheral nervous system is well established, where the channels transmit nociceptive stimuli produced by acidification. ASICs are also expressed in CNS neurons, e.g., in the hippocampus. In cultured hippocampal neurons, ASIC1a was expressed in soma, dendrites, and axons, although synaptic stimulation did not elicit postsynaptic currents mediated by ASICs (Alvarez de la Rosa et al., 2003). ASIC1a is a proton receptor localized on postsynaptic spines and their density is increased after $Ca^{2+}$ elevation and activation of CaMKinase II (Zha, Wemmie, Green, & Welsh, 2006). It is currently thought that ASICs regulate neuronal activity pH-dependently. A role for neuronal ASICs in acidosis-mediated brain injury is now well established, and these channels represent promising novel pharmacological targets for counteracting ischemic brain injury (see Xiong, Pignataro, Li, Chang, & Simon, 2008 review). ASIC expression has also been described in the oligodendrocyte lineage (Feldman et al., 2008) and in NG2 glia (Lin et al., 2015; Lin, Liu, Huang, & Lien, 2010). Moreover, cell culture work suggested expression of ASIC1 in astrocytes (Huang et al., 2010). However, employing freshly isolated astrocytes we did not find ASIC1a, neither on the functional nor on the transcript level, although we confirmed robust expression of ASIC1a/2 in CA1 neurons.

The multisensory transient receptor potential vanilloid type 1 (TRPV1) channel forms an unspecific cationic pore that is also permeable to protons (Hellwig et al., 2004). TRPV1 is mainly located in primary nociceptive neurons and activated by noxious heat, acids, pungent chemicals as well as basic intracellular pH (Dhaka et al., 2009). In addition, it was found in central neurons. In the hippocampus, TRPV1 is located at presynaptic sites in hippocampal CA1 neurons and contributes to synaptic depression

(Gibson, Edwards, Page, Van Hook, & Kauer, 2008), while in the dentate gyrus, TRPV1 receptors mediate synaptic depression of GABAergic neurotransmission onto somata of granule cells (Chavez, Hernandez, Rodenas-Ruano, Chan, & Castillo, 2014). Recent work has implied the presence of TRPV1 in cultured cortical (Huang et al., 2010) and retinal astrocytes, where the channels were activated by mechanical stress and involved in the regulation of migration (Ho, Lambert, & Calkins, 2014). Immunohistochemistry detected TRPV1-positive astrocytic endfeet and pericytes in the hippocampus (Toth et al., 2005), in astrocytic processes in the circumventricular organs (Mannari, Morita, Furube, Tominaga, & Miyata, 2013), and in spinal dorsal horn astrocytes (Doly, Fischer, Salio, & Conrath, 2004). Transcripts encoding TRPV1 were also found in cultured human astrocytes (Amantini et al., 2007). In our study, astrocytes from the hippocampus did not respond to capsaicin, neither did single-cell RT-PCR detect TRPV1 mRNA. Whether these opposing results are due to use of different preparations (culture vs. fresh isolation) or indicative of region-specific astrocytic heterogeneity remains to be determined.

## 4.2 pH Sensitivity of Astrocytes and Its Functional Implications

Astrocytes express different transporters and exchangers which regulate the intracellular pH (Steinhäuser et al., 2013). The electrogenic $Na^+/HCO_3^-$ cotransporter, NBCe1, transports 1 $Na^+$ together with 2 $HCO_3^-$ and can operate in both directions dependent on the actual membrane potential (Deitmer & Schlue, 1989). Knockout studies demonstrated that in astrocytes, extent, and kinetics of recovery from intracellular pH changes largely depend on NBCe1 (Theparambil, Naoshin, Thyssen, & Deitmer, 2015; Theparambil, Ruminot, Schneider, Shull, & Deitmer, 2014). In our experiments, we used nominally $HCO_3^-$ – free HEPES-buffered solutions, but the residual $HCO_3^-$ content might have attenuated intracellular acidification (Theparambil et al., 2014).

In the ventral brainstem, astrocytes may function as $pH/CO_2$-sensors, leading to an elevation of intracellular $Ca^{2+}$ and release of ATP, which activates neurons of the retrotrapezoid nucleus (RTN) and modulates respiratory activity (Gourine et al., 2010). This pH sensitivity of $Ca^{2+}$-dependent astrocytic exocytosis of ATP-filled vesicles is region-specific because it was not observed in cortical astrocytes (Kasymov et al., 2013). The mechanism(s) linking extracellular acidification to elevation of intracellular $Ca^{2+}$ in astrocytes is still under debate. It was suggested that Kir4.1/Kir5.1

heteromeric channels in RTN astrocytes convey pH sensitivity to astrocytes, by depolarizing the cells through block of Kir currents (Wenker et al., 2010). In astrocytes of the nucleus of the solitary tract, depolarization upon inhibition of Kir or background $K^+$ currents compromises glutamate uptake and enhances neuronal excitation (Huda, McCrimmon, & Martina, 2013). Future work has to clarify the molecular basis of astrocytic regulation in respiration and possibly identify new targets for pharmacological intervention in pathological conditions such as decreased respiratory drive or chronic hypercapnia, e.g., chronic obstructive pulmonary disease.

Exposition of cultured astrocytes to low pH, evoked by HCl or lactate, entails a slow drop of intracellular pH and cell death in case of prolonged (hours) application. Both extent and duration of extracellular acidification determine cellular vulnerability. Low intracellular pH affects glycolysis, $Ca^{2+}$ homeostasis, enzymatic activity, gap junction communication, and eventually may induce delayed cell death (Nedergaard et al., 1991; Siesjo et al., 1993). Prolonged oxygen and glucose deprivation are accompanied by altered transmembrane ion gradients can result in reverse operation of the $Na^+$–$H^+$-exchanger and increase the $Ca^{2+}$ load of astrocytes, particularly upon reperfusion (Chesler, 2005), while transient acidification leaves the $Na^+$ gradient intact (Rose et al., 1998). Glial acidosis, induced by oxygen and glucose deprivation or by optogenetic channelrhodopsin-2 activation in astrocytes, activated $Ca^{2+}$-independent glutamate release and triggered excitotoxicity. Accordingly, preventing glial acidosis might serve as a strategy to prevent ischemic brain damage (Beppu et al., 2014).

## 4.3 Kir4.1 as a Therapeutic Target in Neurological Disorders?

Kir channels belong to the superfamily of two-membrane domain channels, lack an intrinsic voltage sensor, and have a high open probability at rest. Inward rectification results from positively charged polyamines and $Mg^{2+}$, which plug the channel from the intracellular site in a voltage-dependent manner. Among the Kir channel family Kir4.1 is expressed in different types of glial cells in the CNS, i.e., astrocytes, oligodendrocytes, NG2 cells, and Müller glial cells (Djukic, Casper, Philpot, Chin, & McCarthy, 2007; Ishii et al., 1997; Seifert et al., 2009; Tang, Taniguchi, & Kofuji, 2009). In astrocytes, Kir4.1 is mainly localized to processes enwrapping synapses and in endfeet around blood vessels (Higashi et al., 2001; Nagelhus, Mathiisen, & Ottersen, 2004). Mice with global or conditional knockout of Kir4.1 developed seizures and died early after birth (Djukic et al., 2007;

Kofuji et al., 2000). Kir4.1-deficient astrocytes have an increased membrane resistance and a depolarized membrane potential (Djukic et al., 2007; Seifert et al., 2009). As a consequence, their ability for $K^+$ buffering and membrane potential-dependent transport, e.g., glutamate uptake, is severely impaired (Djukic et al., 2007; Kucheryavykh et al., 2007). The significance of Kir4.1 in $K^+$ uptake and spatial buffering has been confirmed by experiments showing that its deletion impairs $K^+$ buffering and generates an epileptic phenotype (Chever, Djukic, McCarthy, & Amzica, 2010; Haj-Yasein et al., 2011; Steinhäuser, Seifert, & Bedner, 2012). Under physiological conditions, Kir4.1 regulates synaptic potentiation (Sibille, Pannasch, & Rouach, 2014), extracellular $K^+$ clearance, and membrane potential (Sibille, Dao, Holcman, & Rouach, 2015), particularly during neuronal activity (Larsen et al., 2014; Larsen & MacAulay, 2014).

In humans, mutations in the KCNJ10 gene, which encodes Kir4.1, cause a multiorgan disorder with clinical features of epilepsy, sensorineural deafness, ataxia, and electrolyte imbalance (EAST/SeSAME syndrome; Bockenhauer et al., 2009; Scholl et al., 2009). Single-nucleotide mutations in KCNJ10 cause missense or nonsense mutations on the protein level, and heterologous expression demonstrated that these mutations result in decreased Kir currents and depolarization (Bockenhauer et al., 2009; Reichold et al., 2010; Williams et al., 2010). Furthermore, they increased the pH sensitivity of Kir4.1 and hampered its surface expression (Sala-Rabanal, Kucheryavykh, Skatchkov, Eaton, & Nichols, 2010; Williams et al., 2010). Single-nucleotide variations in the KCNJ10 gene were identified in DNA from patients with temporal lobe epilepsy and hippocampal sclerosis (TLE-HS) or antecedent febrile seizures (Heuser et al., 2010).

Impaired $K^+$ buffering and Kir4.1 expression was observed in hippocampal specimens neurosurgically resected from TLE-HS patients (Steinhäuser et al., 2012). Kir4.1 immunoreactivity was profoundly reduced in perivascular endfeet of astrocytes, and this reduction was accompanied by lower dystrophin labeling suggesting a disruption in the dystrophin-associated protein complex (Heuser et al., 2012). It is important to note that besides impaired Kir4.1 expression, dysfunctional astroglial gap junction coupling is crucial for the impaired $K^+$ clearance as observed in human and experimental TLE-HS (Bedner et al., 2015).

In a mouse model of Huntington's disease, mutant huntingtin protein accumulated in striatal astrocytes and led to decreased Kir4.1 protein and $Ba^{2+}$-sensitive Kir currents, membrane depolarization, and elevated extracellular $K^+$ concentration. In this model, viral delivery of Kir4.1-GFP

rescued Kir4.1 expression in astrocytes and attenuated the phenotype (Tong et al., 2014).

In patients suffering from multiple sclerosis (MS), an inflammatory autoimmune disease, increased titers of serum IgG antibodies against Kir4.1 were observed. Similarly, injection of MS-specific Kir4.1 serum IgG in mice resulted in altered GFAP expression, loss of Kir4.1 and complement deposit in regions of Kir4.1 loss, indicating functional and structural damage in glial cells (Srivastava et al., 2012). In subcortical white matter tissue of autopsies from MS patients, Kir4.1 loss was observed in astrocytic endfeet and oligodendrocytes of demyelinating lesions, while in the periplaque areas Kir4.1 immunoreactivity was retained or even increased (Schirmer et al., 2014). Glial Kir4.1 channels are a primary target of immune responses in MS and display a decreased functionality after injury or in the diseased CNS (Olsen & Sontheimer, 2008; Seifert, Schilling, & Steinhäuser, 2006). They are sensitive to tricyclic antidepressants and to the serotonin reuptake inhibitor fluoxetine. By searching for specific Kir4.1 blockers with functional assays, some amine derivatives were identified that might exert diuretic effects (Raphemot et al., 2013). Neurological disorders would rather benefit from enhanced Kir4.1 function or expression but a drug increasing Kir4.1 function has not yet been identified (Steinhäuser, Grunnet, & Carmignoto, 2015). However, the steroidal hormone β-estradiol turned out to be beneficial after spinal cord injury, by enhancing Kir4.1 expression, glutamate transporters, and improving $K^+$ homeostasis (Olsen, Campbell, McFerrin, Floyd, & Sontheimer, 2010).

## 4.4 Influence of Low Extracellular pH and Ischemia on $K_2P$ Channels in Astrocytes

So far, 15 isoforms of $K_2P$ channels have been identified which are regulated by various stimuli and critically influence the resting membrane potential (Enyedi & Czirjak, 2010). It was suggested that besides Kir4.1, $K_2P$ channels formed by TWIK-1 and TREK-1 contribute to the large $K^+$ conductance of astrocytes and may form heteromeric channels (Hwang et al., 2014; Seifert et al., 2009; Zhou et al., 2009). Our study provides strong evidence for the functional expression of TREK-1 and reveales a parallel developmental regulation of TWIK-1- and TREK-1-encoding transcripts in the hippocampus. Maximal expression was observed 3 weeks after birth, which is in line with previous transcriptome and protein analyses (Cahoy et al., 2008; Wang et al., 2013). Accordingly, Kir4.1 precedes expression of TWIK-1/TREK-1 by about 7 days (Seifert et al., 2009).

TREK-1 expression increases after cerebral ischemia and it was suggested that quinine-sensitive $K^+$ channels, among them TREK-1, stimulate proliferation (Wang et al., 2011). In cell culture, inhibition of TREK-1 channels impairs the clearance of glutamate, both under control and hypoxic conditions. The damage-associated pattern protein (DAMP), S100β, is abundantly expressed by astrocytes and released under hypoxic conditions. Additional block of TREK-1 channels exacerbated S100β secretion (Wu et al., 2013). These results indicate that under hypoxic conditions TREK-1 is activated and, through hyperpolarization, might maintain homeostasis and attenuate DAMP secretion. In cultured astrocytes, TREK-1-mediated currents are sensitive to arachidonic acid, low $pH_i$, and negative pressure (Lu et al., 2014), and our analyses in freshly isolated astrocytes revealed a similar pharmacological profile, assuming that the $pH_o$ changes in our experiments also affected $pH_i$ (Chesler, 2005; Nedergaard et al., 1991). The $pH_i$ regulation *in vivo* is more complex because hypoxia provokes massive changes in transmembrane ionic gradients. Accordingly, results from *in vitro* acidosis may recapitulate only some aspects of systemic ischemia.

In our study, transient application of low $pH_o$-induced inward and outward currents in isolated hippocampal astrocytes, which were insensitive to amiloride. Moreover, capsaicin did not activate responses, indicating that the low $pH_o$-mediated currents were not mediated by TRPV1 or ASIC channels. Another study reported quinine-insensitive $pH_o$-induced currents and suggested that the responses were mediated by yet unknown $K^+$ channels (Chu et al., 2010). However, quinine block of $K_2P$ channels might be impaired at pH 5 due to di-protonation of the tertiary amine nitrogen atoms. Indeed, we observed a loss of quinine sensitivity of $K^+$ channels at pH $<6$ and conclude that the findings of Chu et al. may not exclude functional expression of TREK-1 in astrocytes.

## 4.5 $K_2P$ Channels in Astrocytes as Therapeutic Targets?

Dysfunctional astrocytes are increasingly recognized to contribute to brain pathologies, e.g., to stroke, trauma, inflammation, epilepsy, Alzheimer's disease, and other neurodegenerative diseases, which has raised the question whether these cells might represent new targets for drug development (Lee & MacLean, 2015; Pekny, Wilhelmsson, & Pekna, 2014). Ion channels represent the second largest group of currently used pharmacological targets in neurologic diseases (Overington, Al-Lazikani, & Hopkins, 2006). Their

complex regulation and impact on cellular activity render $K_2P$ channels promising drug targets. Neuroprotective agents such as PUFAs (Blondeau, Widmann, Lazdunski, & Heurteaux, 2002; Fink et al., 1998), riluzole (Duprat et al., 2000), and volatile anesthetics (Patel et al., 1999) are potent activators of TREK-1 and inhibit neuronal excitability. On the other hand, mice with a constitutive knockout of TREK-1 show a higher sensitivity to ischemia, epilepsy, and pain, and the neuroprotective effects of α-linolenic acid or lysophosphatidylcholine are abolished (Alloui et al., 2006; Heurteaux et al., 2004; Noel et al., 2009).

Our present findings confirm and extend previous data on the functional expression of TREK-1 in astrocytes (Hwang et al., 2014; Seifert et al., 2009; Zhou et al., 2009). We show that these glial channels are activated by arachidonic acid, acidification, and membrane crenators mimicking intracellular swelling, i.e., conditions occurring during cerebral ischemia. TREK-1 might be involved in stroke-induced astrogliosis, and hypoxia or acute cerebral ischemia led to upregulation of TREK-1 and astrocytic proliferation (Wang et al., 2011). Systemic administration of riluzole and α-linolenic acid after middle cerebral artery occlusion reduced infarct volume, DNA fragmentation, and cell injury (Heurteaux, Laigle, Blondeau, Jarretou, & Lazdunski, 2006), although the underlying mechanisms and the question whether astrocytes were the primary target of this treatment remained unclear. Similar to Kir channels, TREK-1 contributes to the passive astrocytic membrane conductance and negative resting potential, upon which a number of astrocytic functions depend, including $K^+$ buffering, neurotransmitter uptake, and pH regulation (Olsen & Sontheimer, 2008; Pasler, Gabriel, & Heinemann, 2007). Impaired astrocytic $K^+$ siphoning might be involved in cortical spreading depression observed after traumatic brain injury, migraine, or malignant stroke (reviewed in Torrente et al., 2014). The neuroprotective effect of PUFAs that open TREK-1 channels was demonstrated in an animal model of ischemia and kainate-induced seizures. Intracerebroventricular injection of linolenic acid before induction of ischemia and seizures had a pronounced neuroprotective effect (Lauritzen et al., 2000; reviewed by Mathie & Veale, 2007). However, different problems impede the translation of PUFA for neuroprotection in ischemia and epilepsy. A relatively slow dietary uptake might explain some discrepancies between promising basic research and sobering clinical studies, and ongoing research is looking for increased bioavailability to the brain, e.g., via intravenous administration (Bazinet & Laye, 2014). $K_2P$ channels are ubiquitously expressed by both neurons and glial cells, and their detailed

involvement in the pathogenic events is not well understood. Moreover, the cell types responsible for the observed neuroprotective effects are mostly unknown. Accordingly, additional work is needed to assess the potential of $K_2P$ channels as therapeutic targets.

## ACKNOWLEDGMENT

This work was supported by DFG (STE 552/3), the EU (NSF, EuroEPINOMICS), and BONFOR.

## REFERENCES

Alloui, A., Zimmermann, K., Mamet, J., Duprat, F., Noel, J., Chemin, J., et al. (2006). TREK-1, a K+ channel involved in polymodal pain perception. *EMBO Journal*, *25*, 2368–2376.

Alvarez de la Rosa, D., Krueger, S. R., Kolar, A., Shao, D., Fitzsimonds, R. M., & Canessa, C. M. (2003). Distribution, subcellular localization and ontogeny of ASIC1 in the mammalian central nervous system. *Journal of Physiology*, *546*, 77–87.

Amantini, C., Mosca, M., Nabissi, M., Lucciarini, R., Caprodossi, S., Arcella, A., et al. (2007). Capsaicin-induced apoptosis of glioma cells is mediated by TRPV1 vanilloid receptor and requires p38 MAPK activation. *Journal of Neurochemistry*, *102*, 977–990.

Bazinet, R. P., & Laye, S. (2014). Polyunsaturated fatty acids and their metabolites in brain function and disease. *Nature Reviews Neuroscience*, *15*, 771–785.

Bedner, P., Dupper, A., Huttmann, K., Muller, J., Herde, M. K., Dublin, P., et al. (2015). Astrocyte uncoupling as a cause of human temporal lobe epilepsy. *Brain*, *138*, 1208–1222.

Beppu, K., Sasaki, T., Tanaka, K. F., Yamanaka, A., Fukazawa, Y., Shigemoto, R., et al. (2014). Optogenetic countering of glial acidosis suppresses glial glutamate release and ischemic brain damage. *Neuron*, *81*, 314–320.

Blondeau, N., Widmann, C., Lazdunski, M., & Heurteaux, C. (2002). Polyunsaturated fatty acids induce ischemic and epileptic tolerance. *Neuroscience*, *109*, 231–241.

Bockenhauer, D., Feather, S., Stanescu, H. C., Bandulik, S., Zdebik, A. A., Reichold, M., et al. (2009). Epilepsy, ataxia, sensorineural deafness, tubulopathy, and KCNJ10 mutations. *New England Journal of Medicine*, *360*, 1960–1970.

Cahoy, J. D., Emery, B., Kaushal, A., Foo, L. C., Zamanian, J. L., Christopherson, K. S., et al. (2008). A transcriptome database for astrocytes, neurons, and oligodendrocytes: A new resource for understanding brain development and function. *Journal of Neuroscience*, *28*, 264–278.

Chavez, A. E., Hernandez, V. M., Rodenas-Ruano, A., Chan, C. S., & Castillo, P. E. (2014). Compartment-specific modulation of GABAergic synaptic transmission by TRPV1 channels in the dentate gyrus. *Journal of Neuroscience*, *34*, 16621–16629.

Chesler, M. (2005). Failure and function of intracellular pH regulation in acute hypoxic-ischemic injury of astrocytes. *Glia*, *50*, 398–406.

Chever, O., Djukic, B., McCarthy, K. D., & Amzica, F. (2010). Implication of kir4.1 channel in excess potassium clearance: An in vivo study on anesthetized glial-conditional kir4.1 knock-out mice. *Journal of Neuroscience*, *30*, 15769–15777.

Chu, K. C., Chiu, C. D., Hsu, T. T., Hsieh, Y. M., Huang, Y. Y., & Lien, C. C. (2010). Functional identification of an outwardly rectifying pH- and anesthetic-sensitive leak K(+) conductance in hippocampal astrocytes. *European Journal of Neuroscience*, *32*, 725–735.

Deitmer, J. W., & Schlue, W.-R. (1989). An inwardly directed electrogenic sodium-bicarbonate co-transport in leech glial cells. *Journal of Physiology*, *411*, 179–194.

Dhaka, A., Uzzell, V., Dubin, A. E., Mathur, J., Petrus, M., Bandell, M., et al. (2009). TRPV1 is activated by both acidic and basic pH. *Journal of Neuroscience*, *29*, 153–158.

Djukic, B., Casper, K. B., Philpot, B. D., Chin, L. S., & McCarthy, K. D. (2007). Conditional knock-out of Kir4.1 leads to glial membrane depolarization, inhibition of potassium and glutamate uptake, and enhanced short-term synaptic potentiation. *Journal of Neuroscience*, *27*, 11354–11365.

Doly, S., Fischer, J., Salio, C., & Conrath, M. (2004). The vanilloid receptor-1 is expressed in rat spinal dorsal horn astrocytes. *Neuroscience Letters*, *357*, 123–126.

Duprat, F., Lesage, F., Patel, A. J., Fink, M., Romey, G., & Lazdunski, M. (2000). The neuroprotective agent riluzole activates the two P domain $K^+$ channels TREK-1 and TRAAK. *Molecular Pharmacology*, *57*, 906–912.

Enyedi, P., & Czirjak, G. (2010). Molecular background of leak K+ currents: Two-pore domain potassium channels. *Physiological Reviews*, *90*, 559–605.

Feldman, D. H., Horiuchi, M., Keachie, K., Mccauley, E., Bannerman, P., Itoh, A., et al. (2008). Characterization of acid-sensing ion channel expression in oligodendrocyte-lineage cells. *Glia*, *56*, 1238–1249.

Fink, M., Lesage, F., Duprat, F., Heurteaux, C., Reyes, R., Fosset, M., et al. (1998). A neuronal two P domain K+ channel stimulated by arachidonic acid and polyunsaturated fatty acids. *EMBO Journal*, *17*, 3297–3308.

Gibson, H. E., Edwards, J. G., Page, R. S., Van Hook, M. J., & Kauer, J. A. (2008). TRPV1 channels mediate long-term depression at synapses on hippocampal interneurons. *Neuron*, *57*, 746–759.

Gourine, A. V., Kasymov, V., Marina, N., Tang, F., Figueiredo, M. F., Lane, S., et al. (2010). Astrocytes control breathing through pH-dependent release of ATP. *Science*, *329*, 571–575.

Haj-Yasein, N. N., Jensen, V., Vindedal, G. F., Gundersen, G. A., Klungland, A., Ottersen, O. P., et al. (2011). Evidence that compromised K(+) spatial buffering contributes to the epileptogenic effect of mutations in the human kir4.1 gene (KCNJ10). *Glia*, *59*, 1635–1642.

Hellwig, N., Plant, T. D., Janson, W., Schafer, M., Schultz, G., & Schaefer, M. (2004). TRPV1 acts as proton channel to induce acidification in nociceptive neurons. *Journal of Biological Chemistry*, *279*, 34553–34561.

Heurteaux, C., Guy, N., Laigle, C., Blondeau, N., Duprat, F., Mazzuca, M., et al. (2004). TREK-1, a K+ channel involved in neuroprotection and general anesthesia. *EMBO Journal*, *23*, 2684–2695.

Heurteaux, C., Laigle, C., Blondeau, N., Jarretou, G., & Lazdunski, M. (2006). Alpha-linolenic acid and riluzole treatment confer cerebral protection and improve survival after focal brain ischemia. *Neuroscience*, *137*, 241–251.

Heuser, K., Eid, T., Lauritzen, F., Thoren, A. E., Vindedal, G. F., Tauboll, E., et al. (2012). Loss of perivascular Kir4.1 potassium channels in the sclerotic hippocampus of patients with mesial temporal lobe epilepsy. *Journal of Neuropathology and Experimental Neurology*, *71*, 814–825.

Heuser, K., Nagelhus, E. A., Tauboll, E., Indahl, U., Berg, P. R., Lien, S., et al. (2010). Variants of the genes encoding AQP4 and Kir4.1 are associated with subgroups of patients with temporal lobe epilepsy. *Epilepsy Research*, *88*, 55–64.

Higashi, K., Fujita, A., Inanobe, A., Tanemoto, M., Doi, K., Kubo, T., et al. (2001). An inwardly rectifying K(+) channel, Kir4.1, expressed in astrocytes surrounds synapses and blood vessels in brain. *American Journal of Physiology, Cell Physiology*, *281*, C922–C931.

Ho, K. W., Lambert, W. S., & Calkins, D. J. (2014). Activation of the TRPV1 cation channel contributes to stress-induced astrocyte migration. *Glia*, *62*, 1435–1451.

Honore, E. (2007). The neuronal background K2P channels: Focus on TREK1. *Nature Reviews Neuroscience*, *8*, 251–261.

Huang, C., Hu, Z. L., Wu, W. N., Yu, D. F., Xiong, Q. J., Song, J. R., et al. (2010). Existence and distinction of acid-evoked currents in rat astrocytes. *Glia*, *58*, 1415–1424.

Huda, R., McCrimmon, D. R., & Martina, M. (2013). pH modulation of glial glutamate transporters regulates synaptic transmission in the nucleus of the solitary tract. *Journal of Neurophysiology*, *110*, 368–377.

Hwang, E. M., Kim, E., Yarishkin, O., Woo, D. H., Han, K. S., Park, N., et al. (2014). A disulphide-linked heterodimer of TWIK-1 and TREK-1 mediates passive conductance in astrocytes. *Nature Communications*, *5*, 3227.

Ishii, M., Horio, Y., Tada, Y., Hibino, H., Inanobe, A., Ito, M., et al. (1997). Expression and clustered distribution of an inwardly rectifying potassium channel, KAB-2/Kir4.1, on mammalian retinal Muller cell membrane: Their regulation by insulin and laminin signals. *Journal of Neuroscience*, *17*, 7725–7735.

Julius, D. (2013). TRP channels and pain. *Annual Reviews in Cellular and Developmental Biology*, *29*, 355–384.

Kasymov, V., Larina, O., Castaldo, C., Marina, N., Patrushev, M., Kasparov, S., et al. (2013). Differential sensitivity of brainstem versus cortical astrocytes to changes in pH reveals functional regional specialization of astroglia. *Journal of Neuroscience*, *33*, 435–441.

Kellenberger, S., & Schild, L. (2015). International Union of Basic and Clinical Pharmacology. XCI. Structure, function, and pharmacology of acid-sensing ion channels and the epithelial Na+ channel. *Pharmacological Reviews*, *67*, 1–35.

Kofuji, P., Ceelen, P., Zahs, K. R., Surbeck, L. W., Lester, H. A., & Newman, E. A. (2000). Genetic inactivation of an inwardly rectifying potassium channel (Kir4.1 subunit) in mice: Phenotypic impact in retina. *Journal of Neuroscience*, *20*, 5733–5740.

Kraig, R. P., & Chesler, M. (1990). Astrocytic acidosis in hyperglycemic and complete ischemia. *Journal of Cerebral Blood Flow Metabolism*, *10*, 104–114.

Kucheryavykh, Y. V., Kucheryavykh, L. Y., Nichols, C. G., Maldonado, H. M., Baksi, K., Reichenbach, A., et al. (2007). Downregulation of Kir4.1 inward rectifying potassium channel subunits by RNAi impairs potassium transfer and glutamate uptake by cultured cortical astrocytes. *Glia*, *55*, 274–281.

Larsen, B. R., Assentoft, M., Cotrina, M. L., Hua, S. Z., Nedergaard, M., Kaila, K., et al. (2014). Contributions of the Na(+)/K(+)-ATPase, NKCC1, and Kir4.1 to hippocampal K(+) clearance and volume responses. *Glia*, *62*, 608–622.

Larsen, B. R., & MacAulay, N. (2014). Kir4.1-mediated spatial buffering of K(+): Experimental challenges in determination of its temporal and quantitative contribution to K(+) clearance in the brain. *Channels (Austin.)*, *8*, 544–550.

Lauritzen, I., Blondeau, N., Heurteaux, C., Widmann, C., Romey, G., & Lazdunski, M. (2000). Polyunsaturated fatty acids are potent neuroprotectors. *EMBO Journal*, *19*, 1784–1793.

Lee, K. M., & MacLean, A. G. (2015). New advances on glial activation in health and disease. *World Journal of Virology*, *4*, 42–55.

Lesage, F., & Lazdunski, M. (2000). Molecular and functional properties of two-pore-domain potassium channels. *American Journal of Physiology Renal Physiology*, *279*, F793–F801.

Lin, S. H., Chien, Y. C., Chiang, W. W., Liu, Y. Z., Lien, C. C., & Chen, C. C. (2015). Genetic mapping of ASIC4 and contrasting phenotype to ASIC1a in modulating innate fear and anxiety. *European Journal of Neuroscience*, *41*, 1553–1568.

Lin, Y. C., Liu, Y. C., Huang, Y. Y., & Lien, C. C. (2010). High-density expression of $Ca^{2+}$-permeable ASIC1a channels in NG2 glia of rat hippocampus. *PLoS ONE*, *5*e12665.

Lu, L., Wang, W., Peng, Y., Li, J., Wang, L., & Wang, X. (2014). Electrophysiology and pharmacology of tandem domain potassium channel TREK-1 related BDNF synthesis in rat astrocytes. *Naunyn Schmiedeberg's Archives Pharmacology*, *387*, 303–312.

Maingret, F., Lauritzen, I., Patel, A. J., Heurteaux, C., Reyes, R., Lesage, F., et al. (2000). TREK-1 is a heat-activated background K(+) channel. *EMBO Journal*, *19*, 2483–2491.

Mannari, T., Morita, S., Furube, E., Tominaga, M., & Miyata, S. (2013). Astrocytic TRPV1 ion channels detect blood-borne signals in the sensory circumventricular organs of adult mouse brains. *Glia*, *61*, 957–971.

Mathie, A., & Veale, E. L. (2007). Therapeutic potential of neuronal two-pore domain potassium-channel modulators. *Current Opinion in Investigational Drugs*, *8*, 555–562.

Matthias, K., Kirchhoff, F., Seifert, G., Hüttmann, K., Matyash, M., Kettenmann, H., et al. (2003). Segregated expression of AMPA-type glutamate receptors and glutamate transporters defines distinct astrocyte populations in the mouse hippocampus. *Journal of Neuroscience*, *23*, 1750–1758.

Miller, P., Kemp, P. J., Lewis, A., Chapman, C. G., Meadows, H. J., & Peers, C. (2003). Acute hypoxia occludes hTREK-1 modulation: Re-evaluation of the potential role of tandem P domain K+ channels in central neuroprotection. *Journal of Physiology*, *548*, 31–37.

Nagelhus, E. A., Mathiisen, T. M., & Ottersen, O. P. (2004). Aquaporin-4 in the central nervous system: Cellular and subcellular distribution and coexpression with KIR4.1. *Neuroscience*, *129*, 905–913.

Nedergaard, M., Goldman, S. A., Desai, S., & Pulsinelli, W. A. (1991). Acid-induced death in neurons and glia. *Journal of Neuroscience*, *11*, 2489–2497.

Noel, J., Zimmermann, K., Busserolles, J., Deval, E., Alloui, A., Diochot, S., et al. (2009). The mechano-activated K+ channels TRAAK and TREK-1 control both warm and cold perception. *EMBO Journal*, *28*, 1308–1318.

Nolte, C., Matyash, M., Pivneva, T., Schipke, C. G., Ohlemeyer, C., Hanisch, U. K., et al. (2001). GFAP promoter-controlled EGFP-expressing transgenic mice: A tool to visualize astrocytes and astrogliosis in living brain tissue. *Glia*, *33*, 72–86.

Olsen, M. L., Campbell, S. C., McFerrin, M. B., Floyd, C. L., & Sontheimer, H. (2010). Spinal cord injury causes a wide-spread, persistent loss of Kir4.1 and glutamate transporter 1: Benefit of 17 beta-oestradiol treatment. *Brain*, *133*, 1013–1025.

Olsen, M., & Sontheimer, H. (2008). Functional implications for Kir4.1 channels in glial biology: From K+ buffering to cell differentiation. *Journal of Neurochemistry*, *107*, 589–601.

Overington, J. P., Al-Lazikani, B., & Hopkins, A. L. (2006). How many drug targets are there? *Nature Reviews Drug Discovery*, *5*, 993–996.

Pasler, D., Gabriel, S., & Heinemann, U. (2007). Two-pore-domain potassium channels contribute to neuronal potassium release and glial potassium buffering in the rat hippocampus. *Brain Research*, *1173*, 14–26.

Patel, A. J., Honoré, E., Lesage, F., Fink, M., Romey, G., & Lazdunski, M. (1999). Inhalational anesthetics activate two-pore-domain background $K^+$ channels. *Nature Neuroscience*, *2*, 422–426.

Pekny, M., Wilhelmsson, U., & Pekna, M. (2014). The dual role of astrocyte activation and reactive gliosis. *Neuroscience Letters*, *565*, 30–38.

Pessia, M., Imbrici, P., D'Adamo, M. C., Salvatore, L., & Tucker, S. J. (2001). Differential pH sensitivity of Kir4.1 and Kir4.2 potassium channels and their modulation by heteropolymerisation with Kir5.1. *Journal of Physiology*, *532*, 359–367.

Raphemot, R., Kadakia, R. J., Olsen, M. L., Banerjee, S., Days, E., Smith, S. S., et al. (2013). Development and validation of fluorescence-based and automated patch clamp-based functional assays for the inward rectifier potassium channel Kir4.1. *Assay and Drug Development Technology*, *11*, 532–543.

Rehncrona, S. (1985). Brain acidosis. *Annals of Emergency Medicine*, *14*, 770–776.

Reichold, M., Zdebik, A. A., Lieberer, E., Rapedius, M., Schmidt, K., Bandulik, S., et al. (2010). KCNJ10 gene mutations causing EAST syndrome (epilepsy, ataxia, sensorineural deafness, and tubulopathy) disrupt channel function. *Proceedings of the National Academy of Sciences USA*, *107*, 14490–14495.

Rose, C. R., Waxman, S. G., & Ransom, B. R. (1998). Effects of glucose deprivation, chemical hypoxia, and simulated ischemia on $Na^+$ homeostasis in rat spinal cord astrocytes. *Journal of Neuroscience*, *18*, 3554–3562.

Sala-Rabanal, M., Kucheryavykh, L. Y., Skatchkov, S. N., Eaton, M. J., & Nichols, C. G. (2010). Molecular mechanisms of EAST/SeSAME syndrome mutations in Kir4.1 (KCNJ10). *Journal of Biological Chemistry*, *285*, 36040–36048.

Sandoz, G., Douguet, D., Chatelain, F., Lazdunski, M., & Lesage, F. (2009). Extracellular acidification exerts opposite actions on TREK1 and TREK2 potassium channels via a single conserved histidine residue. *Proceedings of the National Academy of Sciences USA*, *106*, 14628–14633.

Schirmer, L., Srivastava, R., Kalluri, S. R., Bottinger, S., Herwerth, M., Carassiti, D., et al. (2014). Differential loss of KIR4.1 immunoreactivity in multiple sclerosis lesions. *Annals of Neurology*, *75*, 810–828.

Scholl, U. I., Choi, M., Liu, T., Ramaekers, V. T., Hausler, M. G., Grimmer, J., et al. (2009). Seizures, sensorineural deafness, ataxia, mental retardation, and electrolyte imbalance (SeSAME syndrome) caused by mutations in KCNJ10. *Proceedings of the National Academy of Science USA*, *106*, 5842–5847.

Seifert, G., Hüttmann, K., Binder, D. K., Hartmann, C., Wyczynski, A., Neusch, C., et al. (2009). Analysis of astroglial $K^+$ channel expression in the developing hippocampus reveals a predominant role of the Kir4.1 subunit. *Journal of Neuroscience*, *29*, 7474–7488.

Seifert, G., Rehn, L., Weber, M., & Steinhäuser, C. (1997). AMPA receptor subunits expressed by single astrocytes in the juvenile mouse hippocampus. *Molecular Brain Research*, *47*, 286–294.

Seifert, G., Schilling, K., & Steinhäuser, C. (2006). Astrocyte dysfunction in neurological disorders: A molecular perspective. *Nature Reviews Neuroscience*, *7*, 194–206.

Seifert, G., & Steinhäuser, C. (1995). Glial cells in the mouse hippocampus express AMPA receptors with an intermediate $Ca^{2+}$ permeability. *European Journal of Neuroscience*, *7*, 1872–1881.

Sibille, J., Dao, D. K., Holcman, D., & Rouach, N. (2015). The neuroglial potassium cycle during neurotransmission: Role of Kir4.1 channels. *PLoS Computational Biology*, *11*, e1004137.

Sibille, J., Pannasch, U., & Rouach, N. (2014). Astroglial potassium clearance contributes to short-term plasticity of synaptically evoked currents at the tripartite synapse. *Journal of Physiology*, *592*, 87–102.

Siesjo, B. K., Katsura, K., Mellergard, P., Ekholm, A., Lundgren, J., & Smith, M. L. (1993). Acidosis-related brain damage. *Progress in Brain Research*, *96*, 23–48.

Srivastava, R., Aslam, M., Kalluri, S. R., Schirmer, L., Buck, D., Tackenberg, B., et al. (2012). Potassium channel KIR4.1 as an immune target in multiple sclerosis. *New England Journal of Medicine*, *367*, 115–123.

Steinhäuser, C., Grunnet, M., & Carmignoto, G. (2015). Crucial role of astrocytes in temporal lobe epilepsy. *Neuroscience*. http://dx.doi.org/10.1016/j.neuroscience.2014.12.047.

Steinhäuser, C., Seifert, G., & Bedner, P. (2012). Astrocyte dysfunction in temporal lobe epilepsy: K+ channels and gap junction coupling. *Glia*, *60*, 1192–1202.

Steinhäuser, C., Seifert, G., & Deitmer, J. W. (2013). Physiology of astrocytes: Ion channels and transporters. In H. Kettenmann & B. Ransom (Eds.), *Neuroglia*. (3rd ed.). New York, USA: Oxford University Press.

Tang, X., Taniguchi, K., & Kofuji, P. (2009). Heterogeneity of Kir4.1 channel expression in glia revealed by mouse transgenesis. *Glia*, *57*, 1706–1715.

Theparambil, S. M., Naoshin, Z., Thyssen, A., & Deitmer, J. W. (2015). Reversed electrogenic sodium bicarbonate cotransporter 1 is the major acid loader during recovery from cytosolic alkalosis in mouse cortical astrocytes. *Journal of Physiology*, *593*, 3533–3547.

Theparambil, S. M., Ruminot, I., Schneider, H. P., Shull, G. E., & Deitmer, J. W. (2014). The electrogenic sodium bicarbonate cotransporter NBCe1 is a high-affinity bicarbonate carrier in cortical astrocytes. *Journal of Neuroscience*, *34*, 1148–1157.

Tong, X., Ao, Y., Faas, G. C., Nwaobi, S. E., Xu, J., Haustein, M. D., et al. (2014). Astrocyte Kir4.1 ion channel deficits contribute to neuronal dysfunction in Huntington's disease model mice. *Nature Neuroscience*, *17*, 694–703.

Torrente, D., Cabezas, R., Avila, M. F., Garcia-Segura, L. M., Barreto, G. E., & Guedes, R. C. (2014). Cortical spreading depression in traumatic brain injuries: Is there a role for astrocytes? *Neuroscience Letters*, *565*, 2–6.

Toth, A., Boczan, J., Kedei, N., Lizanecz, E., Bagi, Z., Papp, Z., et al. (2005). Expression and distribution of vanilloid receptor 1 (TRPV1) in the adult rat brain. *Molecular Brain Research*, *135*, 162–168.

Waldmann, R., Champigny, G., Bassilana, F., Heurteaux, C., & Lazdunski, M. (1997). A proton-gated cation channel involved in acid-sensing. *Nature*, *386*, 173–177.

Wallraff, A., Kohling, R., Heinemann, U., Theis, M., Willecke, K., & Steinhäuser, C. (2006). The impact of astrocytic gap junctional coupling on potassium buffering in the hippocampus. *Journal of Neuroscience*, *26*, 5438–5447.

Wang, W., Putra, A., Schools, G. P., Ma, B., Chen, H., Kaczmarek, L. K., et al. (2013). The contribution of TWIK-1 channels to astrocyte K(+) current is limited by retention in intracellular compartments. *Frontiers in Cellular Neuroscience*, 7, 246.

Wang, M., Song, J., Xiao, W., Yang, L., Yuan, J., Wang, W., et al. (2011). Changes in lipid-sensitive two-pore domain potassium channel TREK-1 expression and its involvement in astrogliosis following cerebral ischemia in rats. *Journal of Molecular Neuroscience*, *46*, 384–392.

Wenker, I. C., Kreneisz, O., Nishiyama, A., & Mulkey, D. K. (2010). Astrocytes in the retrotrapezoid nucleus sense H+ by inhibition of a Kir4.1-Kir5.1-like current and may contribute to chemoreception by a purinergic mechanism. *Journal of Neurophysiology*, *104*, 3042–3052.

Williams, D. M., Lopes, C. M., Rosenhouse-Dantsker, A., Connelly, H. L., Matavel, A., Uchi, J., et al. (2010). Molecular basis of decreased Kir4.1 function in SeSAME/EAST syndrome. *Journal of the American Society of Nephrology*, *21*, 2117–2129.

Woo, D. H., Han, K. S., Shim, J. W., Yoon, B. E., Kim, E., Bae, J. Y., et al. (2012). TREK-1 and Best1 channels mediate fast and slow glutamate release in astrocytes upon GPCR activation. *Cell*, *151*, 25–40.

Wu, X., Liu, Y., Chen, X., Sun, Q., Tang, R., Wang, W., et al. (2013). Involvement of TREK-1 activity in astrocyte function and neuroprotection under simulated ischemia conditions. *Journal of Molecular Neuroscience*, *49*, 499–506.

Xiong, Z. G., Pignataro, G., Li, M., Chang, S. Y., & Simon, R. P. (2008). Acid-sensing ion channels (ASICs) as pharmacological targets for neurodegenerative diseases. *Current Opinion in Pharmacology*, *8*, 25–32.

Zha, X. M., Wemmie, J. A., Green, S. H., & Welsh, M. J. (2006). Acid-sensing ion channel 1a is a postsynaptic proton receptor that affects the density of dendritic spines. *Proceedings of the National Academy of Sciences USA*, *103*, 16556–16561.

Zhou, M., Xu, G., Xie, M., Zhang, X., Schools, G. P., Ma, L., et al. (2009). TWIK-1 and TREK-1 are potassium channels contributing significantly to astrocyte passive conductance in rat hippocampal slices. *Journal of Neuroscience*, *29*, 8551–8564.

## 3. Danksagung

Ich möchte mich herzlich bei allen Menschen bedanken, die mich bei der Erstellung dieser Arbeit unterstützt haben.

Insbesondere möchte ich mich bei meinem Doktorvater Prof. Dr. Steinhäuser für die Überlassung des Themas, die Betreuung und die Gewährung der ausgezeichneten Möglichkeiten zur Bearbeitung der Fragestellung sowie die wertvolle und geduldige Unterstützung bedanken. Prof. Dr. Steinhäuser hat mir die Möglichkeit gegeben, meine Promotion in einer motivierenden und wissenschaftlich orientierten Umgebung durchzuführen.

Mein besonderer Dank gebührt meinem Betreuer und Arbeitsgruppenleiter PD Dr. Seifert, der mir mit Betreuung, tatkräftiger Unterstützung und Fachwissen stets zur Seite stand.

Des Weiteren danke ich allen Mitarbeitern des Instituts für Zelluläre Neurowissenschaften für wertvolle Anregungen, die stete Hilfsbereitschaft sowie die gute Arbeitsatmosphäre.

Bedanken möchte ich mich bei BONFOR für die ideelle und materielle Unterstützung meines Forschungsvorhabens. Weiterhin gilt mein Dank Frau Cieslak vom Promotionsbüro für die Unterstützung in der letzten Phase der Arbeit.

Nicht zuletzt danke ich vor allem meinen Eltern, die in jeglicher Hinsicht die Grundsteine für meinen Weg gelegt haben und mich immer unterstützen.